

# Market and system security impact of the storm demonstration in task-forces TF2. Deliverable: D16.6

WP16. EU wide integrating assessment of demonstration replication potential

**Cutululis, Nicolaos Antonio; Altiparmakis, Argyrios; Litong-Palima, Marisciel; Detlefsen, Nina ; Sørensen, Poul Ejnar**

*Publication date:*
2013

*Document Version*
Publisher's PDF, also known as Version of record

# Market and system security impact of the storm demonstration in task-forces TF2

Deliverable: D16.6

EC-GA nº 249812

**Project full title:** Transmission system operation with large penetration of Wind and other renewable Electricity sources in Networks by means of innovative Tools and Integrated Energy Solutions

## Document info

| | |
|---|---|
| Document Name | Market impact of the storm demonstration in task-forces TF2 |
| Responsible Partner | DTU |
| Work Package | WP16. EU wide integrating assessment of demonstration replication potential |
| Deliverable nº : | D16.6 |
| Authors: | Nicolaos A. Cutululis, DTU<br>Argyrios Altiparmakis, DTU<br>Marisciel Litong-Palima, DTU<br>Nina Detlefsen, Energinet.dk<br>Poul Sørensen, DTU |
| WP leader | Poul Sørensen, DTU |
| Approvals: | TWENTIES Technical Committee |

## Disclaimer

This document has been prepared by TWENTIES project partners as an account of work carried out within the framework of the EC-GA contract nº 249812.

Neither Project Coordinator, nor any signatory party of TWENTIES Project Consortium Agreement, nor any person acting on behalf of any of them:

(a) makes any warranty or representation whatsoever, express or implied,

(i) with respect to the use of any information, apparatus, method, process, or similar item disclosed in this document, including merchantability and fitness for a particular purpose, or

(ii) that such use does not infringe on or interfere with privately owned rights, including any party's intellectual property, or

(iii) that this document is suitable to any particular user's circumstance; or assumes responsibility for any damages or other liability whatsoever (including any consequential damages, even if Project Coordinator or any representative of a signatory party of the TWENTIES Project Consortium Agreement, has been advised of the possibility of such damages) resulting from your selection or use of this document or any information, apparatus, method, process, or similar item disclosed in this document.

# TABLE OF CONTENTS

## Executive summary

A survey of the plans for offshore wind power development in northern Europe – including the North and Baltic Seas – has estimated that there could be 40 GW by 2020 and 114 GW by 2030. Simulation of wind power time series with this spatial concentration of large-scale wind power show that the variability of wind power will increase significantly in the European power systems. The figure below shows an example of how a new High Wind Extended Power (HWEP) such as SIEMENS HWRT™ controller used in Demo 4 will reduce the wind power ramp rates during storms compared to the old HWSD controller which was used offshore until now.

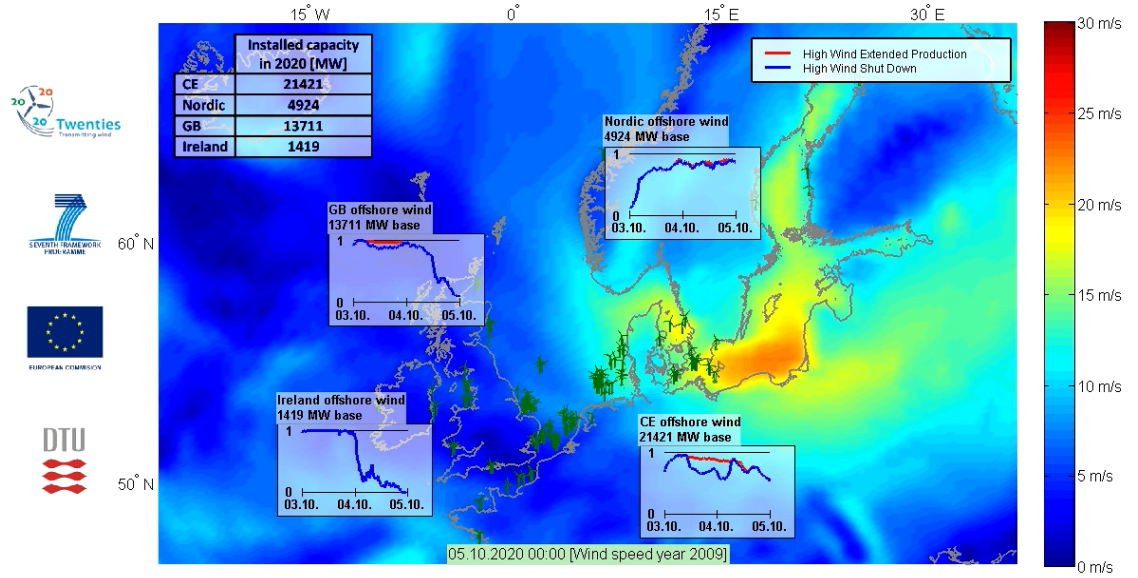


Based on eight years of meteorological data, the maximum 15 minute ramp rates have been calculated with both storm controllers in each synchronous area as a measure for needed frequency containment reserves. The results show a significant increase in the maximum ramp rates from 2020 to 2030. The effect of the storm controller is visible, but not very significant when looking at the large synchronous areas.

Wind power forecast errors can be significantly reduced in storm periods, especially on a national level, by high wind ride through controls. At European level, the impact is less significant, but can reduce the volume of frequency containment reserves needed to ensure secure system operation

Increasing both the hydro capacity and the interconnection capacities has a benefic impact on the overall system. The costs are reduced by a little more than 0,5 B€. The CO2 emissions are also reduced with 10 mil tonnes. Finally, wind power curtailment is reduced with app. 1,5 TWh/year.

The use of the new storm controller has a positive impact of the overall system. First of all, the wind power production is increased with more than 4TWh/year, even some of it is curtailed. In terms of costs, the overall system costs are reduced with app. 100 M€ and the CO2 emissions are reduced with 1 MTonne.

# 1. Introduction

This document presents the deliverable D16.6, which is one of the three deliverables contained in WP 16 as stated in the DoW:

**Table 1 Description of deliverable in DoW WP16**

| **Deliverables:** | | | |
|---|---|---|---|
| **D16.6** | (DTU) | Report on market impact | M36 (Mar-13) |

This report quantifies the variability of the offshore wind power planned in North Europe by 2020 and 2030, taking into account the fast variability down to the minute time scale and the effect of the demonstrated storm controls. In Tradewind and other wind power integration studies, wind power has been represented by historical data and by Reanalysis data, which underestimates the offshore wind power variability significantly. Concerning historical wind power data, the experience with large offshore wind farms so far has clearly shown that the offshore wind power is significantly more variable than the on-shore wind power, first of all because offshore wind power is more concentrated geographically than existing on-shore wind power. The reanalysis data has also been shown to underestimate the wind power variability, typically in the time scale from minutes up to one day. In this view, DTU Wind has developed CorWind simulation model, which enables simulations of wind power time series, using Reanalysis data to provide the slow wind variability and adding the faster variability by a stochastic model. Both the reanalysis model and the stochastic model in WPTS take into account the correlation between wind speeds at neighbouring locations, and the phase delay of the wind speed variation in the wind direction.

The importance of different developments in European offshore wind power and availability of flexible hydropower resources for the costs of the power system are quantified in the report. The Wilmar Planning tool is used to quantify the operational costs.

Besides the market impact of offshore wind power development, Nordic hydro power plant capacity and grid constraints, the report quantifies the offshore wind power variability and compares it to the reference incident used to determine the need for frequency containment reserves in the relevant synchronous areas.

## 2. Simulation of wind power time series

The analysis done in this report is focusing on synchronous areas rather than countries. This is because wind power variability will mainly affect the frequency, which is the same for the whole synchronous area, hence a country-wise analysis would be rather redundant.

The simulations are based on the offshore wind power development scenarios presented in [1]. While individual offshore wind farms are simulated, the analysis was done per synchronous areas, since the variability introduced by wind should be dealt with at system level. The synchronous areas considered in the analysis are: Continental, Nordic, Great Britain and Ireland. The installed capacities, per area, in 2020 and 2030 are given in Table 2.1:

**Table 2.1** Wind power capacities considered in the scenarios, per synchronous areas

| Synchronous Area | 2020 | 2030 |
|---|---|---|
| | **MW** | **MW** |
| **Continental** | 21,432 | 54,187 |
| **Nordic** | 4,913 | 14,798 |
| **GB** | 13,711 | 33,601 |
| **Ireland** | 1,419 | 4,319 |

The geographical distribution of the offshore wind farms considered in the analysis is shown in Figure 1 for 2020 and in Figure 2 for 2030, respectively. The circles are scaled with the installed capacity

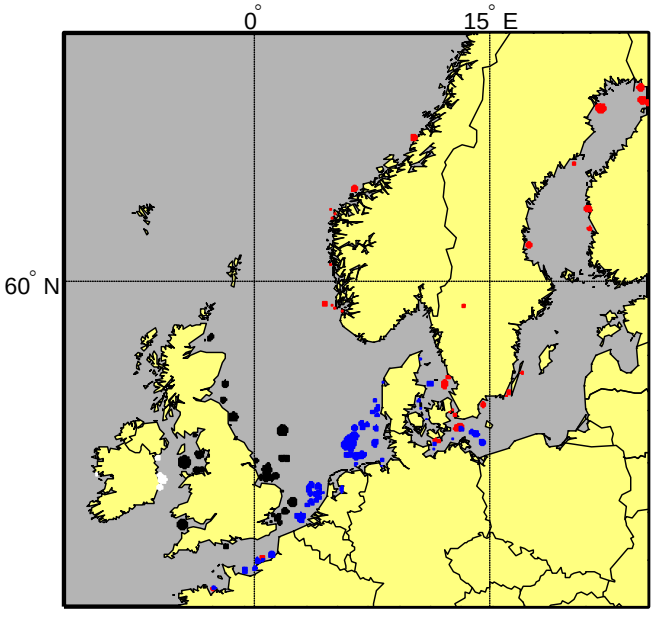


**Figure 1** Offshore wind farms per synchronous system – 2020 (Continental – blue, Nordic – red, GB – black and Ireland – white)

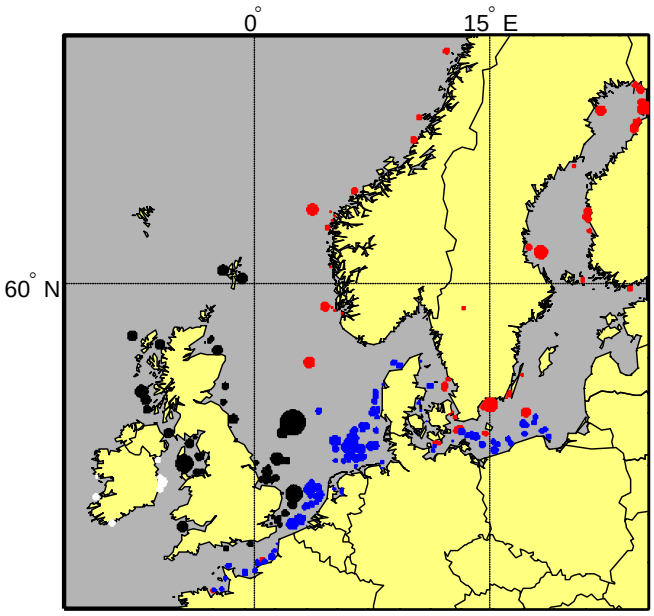


**Figure 2** Offshore wind farms per synchronous system – 2030 (Continental – blue, Nordic – red, GB – black and Ireland – white)

In the analysis presented in this report, a total of eight meteorological (or wind speed) years were used in the simulations. The selection was done taking into account the existence of data (see §2.1), the number of very high wind events recorded and the need of different, i.e. "good" or "average", etc, wind years. In the following, we refer to the years as Meteo Years from 1 to 8. Their correspondence with calendar years is given in Table 2.2.

**Table 2.2** Correspondence between meteo and calendar years

| Meteo Year | Calendar Year |
|---|---|
| **1** | 2001 |
| **2** | 2005 |
| **3** | 2007 |
| **4** | 2008 |
| **5** | 2009 |
| **6** | 2010 |
| **7** | 2011 |
| **8** | 2012 |

## 2.1. Tools

***CorWind***

The CORrelated WIND power fluctuations (CorWind) model has been developed at DTU Wind Energy (former Risø) for over a decade now. It is a software tool that allows the simulation of wind power time series that have a realistic variability. Furthermore, CorWind can simulate wind power output in different locations, taking into account the spatial correlation between them.

CorWind is an extension of the linear and purely stochastic PARKSIMU model [9] which simulates stochastic wind speed time series for individual wind turbines in a wind farm, with fluctuations of each time series according to specified power spectral densities and with correlations between the different wind turbine time series according to specified coherence functions. The coherence functions depend on frequency and space, ensuring that the correlation between two wind speed time series will decrease with increasing distance between the points. Moreover, the slow wind speed fluctuations are more correlated than the fast fluctuations. Finally, the stochastic PARKSIMU model includes the phase shift between correlated waves in downstream points, ensuring that correlated wind speed variations will be delayed in time as they travel through the wind farm. These model properties ensure that the summed power from multiple wind turbines will have realistic fluctuations, which has been validated using measured time series of simultaneous wind speeds and power from individual wind turbines in two large wind farms in Denmark.

The CorWind extension of PARKSIMU is intended to allow simulations over large areas and long time periods. The linear approach applied in PARKSIMU assumes constant mean wind speeds and constant mean wind directions during a simulation period, which limits the geographical area as well as the simulation period significantly–typically to the area of a single wind farm and to a maximum period of two hours. CorWind uses reanalysis data from a climate model to provide the mean wind flow over a large region, and then adds a stochastic contribution using an adapted version of the PARKSIMU approach that allows the mean flow to vary in time and space.

The meteorological data was produced using a mesoscale reanalysis method, which is often used for obtaining high-resolution climate or climate change information from relatively coarse-resolution global general circulation models or reanalysis. The mesoscale reanalysis uses a limited-area, high-resolution model driven by boundary conditions from the reanalysis. The strength in using the models to fill the observation gaps is that the fields are dynamically consistent and they are defined on a regular grid. Additionally, the models respond to local forcing that adds information beyond what can be represented by the observations.

The mesoscale reanalysis used to generate the meteorological time series uses the National Center for Atmospheric Research (NCAR) Advanced Research Weather Research and Forecasting (ARW-WRF) model [10]. The version used is v3.2.1 that was released 18 August 2010. The model forecasts use 41 vertical levels from the surface to the top of the model located at 50 HPa; 12 of these levels are placed within 1000 m of the surface. The model setup uses standard physical parameterizations including the Mellor-Yamada (MYJ) PBL scheme [11].

The model was integrated within the domain shown in Figure 3. The model grid has a horizontal spacing of 30 km, on a polar stereographic projection with center at 52.2°N, 10°E. The domain has dimensions of 115 × 108. The simulation from which the meteorological time series are derived covers twelve years (2000–2011). Individual runs are re-initialized every 11

days. Each run overlaps the previous one by 24 h, to avoid using the time during which the model is spinning up mesoscale processes. A similar method was used and verified in [12]-[14]. Initial boundary and grids for nudging are supplied by the ERA Interim Reanalysis [15].

The model was validated against measurements from the two largest – at the time – offshore wind farms in the world, namely Horns Rev 1 wind farm located in the North Sea in the west coast of Denmark and Nysted wind farm, located in the south coast of Denmark, in the Baltic sea.

The validation was done in terms of wind farm ramp rates. The measured wind farm power is calculated in p.u. as the average power of the available turbines in each 2 hour segment. Thus, the reduction of the wind farm power due to non availability of wind turbines is removed. This choice is justified because missing data from a turbine is not necessarily indicating that the turbine is not producing power, but can also be because of failures in the SCADA system.

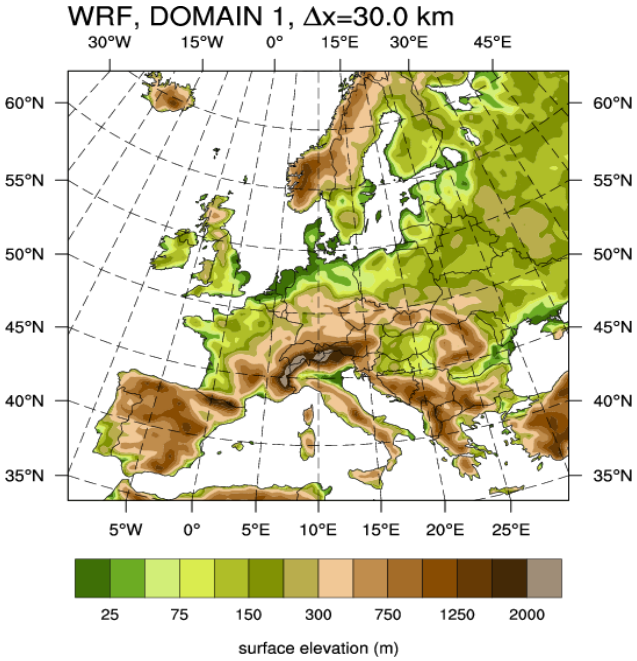


**Figure 3** Domain configuration and terrain elevation used in the simulations for domain (30 km)

For each measured 2 hour segment, the average wind speed and wind direction is calculated, and a 2 hour wind farm power time series is simulated. The simulations are performed with the detailed model including low frequency fluctuations and wind farm generated turbulence.

When the ramp rates have been calculated for each set of neighbour periods $n$ and $n$+1 for all segments, the ramp rates are binned according the corresponding initial power $P_{mean}(n)$. This is because the statistics of the ramping will depend strongly on the initial power. For instance, the power is not likely to increase very much when it is already close to rated. A power bins size 0.1 p.u. has been selected.

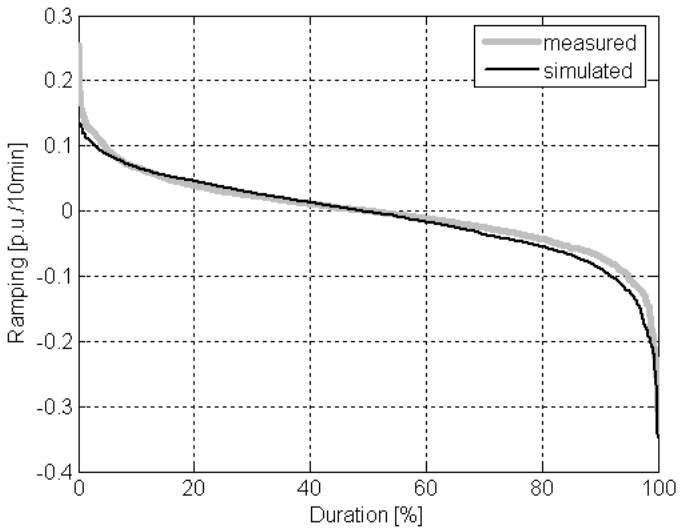


**Figure 4** Duration curves of 10 minutes ramp rates in the initial power range from 0.8 to 0.9 p.u.

The ramping is sorted in each power bin, and a duration curve is obtained. This is done for the measurements and for the simulations. As an example, the duration curves for ten minute ramp rates in the initial power range between 0.8 - 0.9 p.u. is shown in Figure 4. There is a good agreement between the simulated and the measured duration curves.

The most interesting point of the duration curves is the highest wind farm negative ramp rate, i.e. around 100% on the duration curve, because this quantifies the highest requirement to the ramp rates of other power plants. The wind farm positive ramp rates are not so interesting here because they can be limited directly by the wind farm main controller.

In Figure 5, the 99% percentile of the 10 minutes ramp rates duration curve for all power ranges is shown. In order to assess the model performances, both Horns Rev and Nysted simulated and measured ramp rates are plotted.

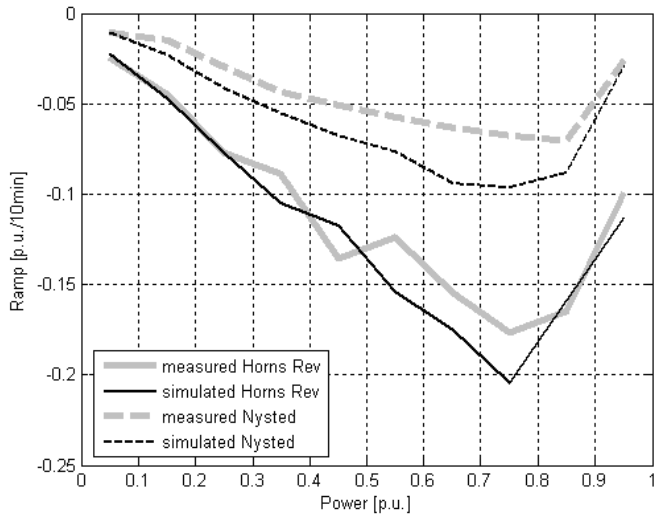


**Figure 5** The 99% percentiles of 10 minutes ramp rates in all power ranges for Horns Rev 1 and Nysted wind farm

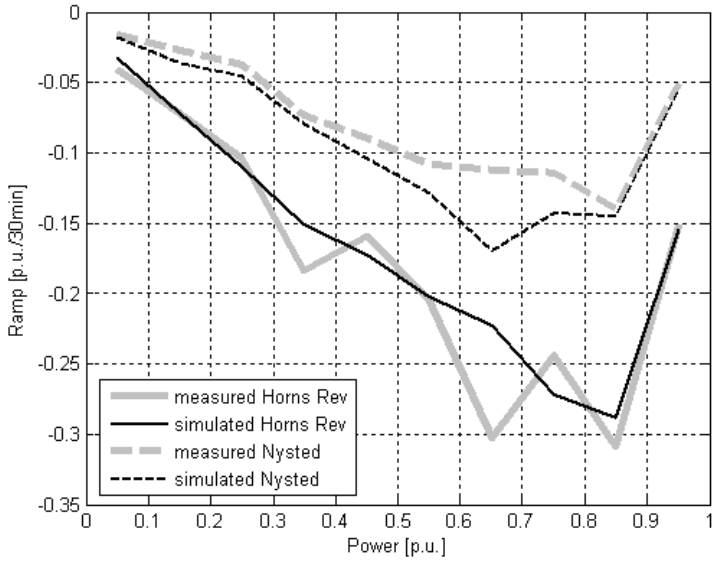


**Figure 6** The 99% percentiles of 30 minutes ramp rates in all power ranges for Horns Rev and Nysted wind farms

The 99% percentile for 30 minutes period is shown in Figure 6. The match between simulated and measured power fluctuations is similar to the 10 minutes periods, with the simulated power fluctuations still being systematically bigger than the measured ones.

**Wind2Power module**

The Wind2Power module does, as the name suggests, the conversion from wind speed to power. This conversion can be done using the so-called power curve, which is the characteristic curve that describes the relationship between the wind speed and power. In this study, our interest lies in simulating the power production in the synchronous areas in Northern Europe for all the probable values of the wind speed, from the low level all the way up to the high level, i.e. during storms. Before we can do this, we first needed to validate our tools at the turbine and at the farm levels.

We considered two cases of storm control for the turbine, corresponding to the HWSD and HWEP cases as shown in Figure 7 and the Figure 8, respectively. As suggested in the figures, the turbine can shutdown whenever one of the three speed averages, which are the ones computed over 10minutes, 30seconds and 1 second, exceed their specified limits. Also, for both cases, the turbines are restarted once the 10min wind speed average dips below 20m/s. Note that the speed limits that are specified for the HWEP case are correspondingly higher than for the HWSD case. In effect, when a turbine is used with the HWEP control, it is less likely to shutdown due to high and rare wind speed levels and so it would most likely operate through a storm event, albeit at a power output that is reduced from the rated level.

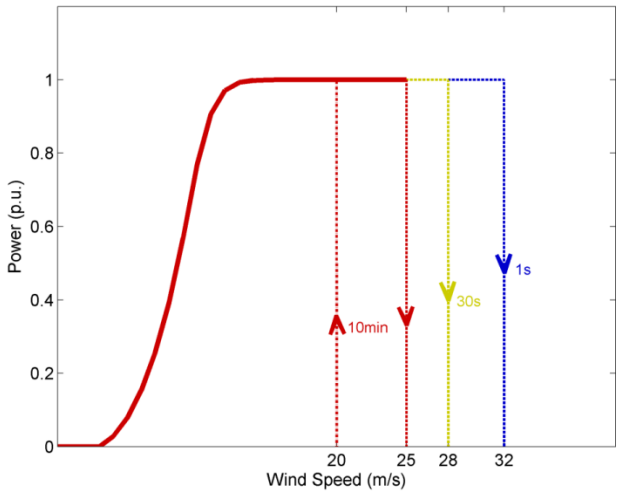


**Figure 7** The power curve of an individual turbine for the HWSD case.

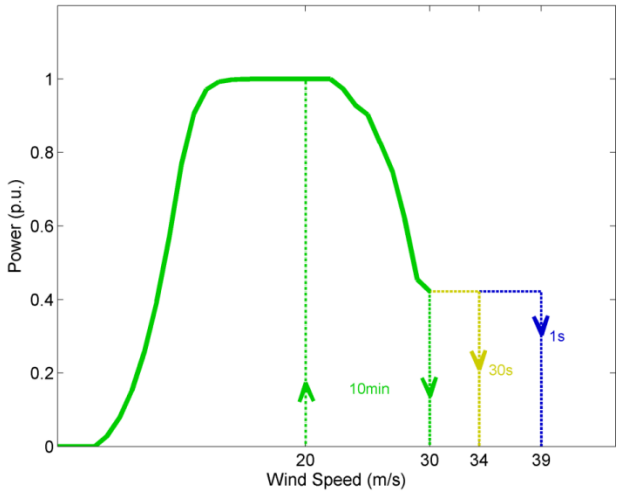


**Figure 8** The power curve of an individual turbine for the HWEP case.

The power curve is given for a single wind turbine hence using it directly implies simulating each individual wind turbine, in each simulated wind power plant. This is achievable when the focus is on one or few wind power plants, summing up to a few hundreds wind turbines. In this work, the focus is on the entire North Europe and to an installed capacity of more than 140GW in the 2030 scenario, divided across almost 400 wind power plants [1]. This meant that it was needed to derive an aggregated wind power plant power curve. The exercise started with a generic 200MW wind power plant power curve available at DTU Wind Energy and validated against measurements from Horns Rev 2 wind power plant in Denmark. The results of this farm-level validation is shown in Figure 9 for the HWSD case and Figure 10 for the HWEP case.

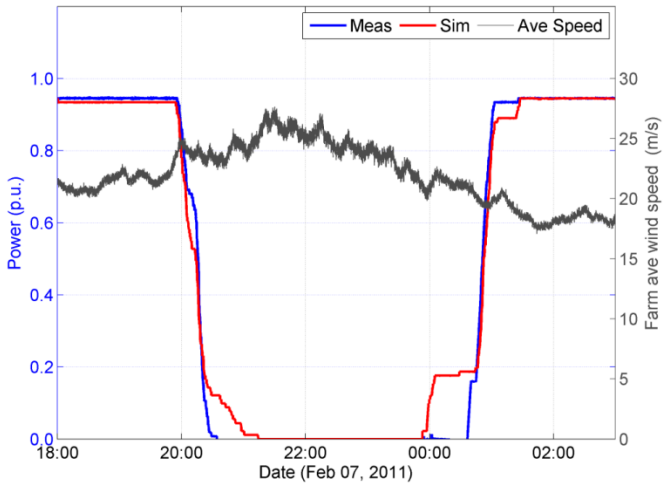


**Figure 9** Validation of Storm control algorithm by comparing simulated against measured power for the HWSD case.

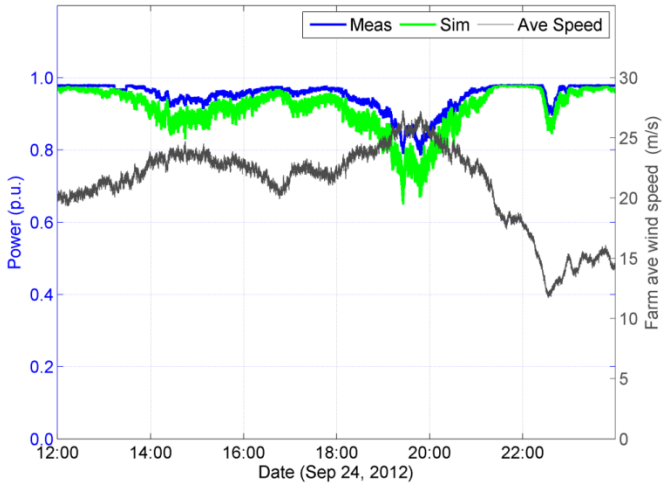


**Figure 10** Validation of Storm control algorithm by comparing simulated against measured power for the HWSD case

The Wind2Power module of CorWind is then updated to run the two cases of storm control. After this validation, CorWind is used to estimate the aggregated power curve for Horns Rev2

wind farm. The estimation of the aggregated power curve is illustrated in Figure 11.

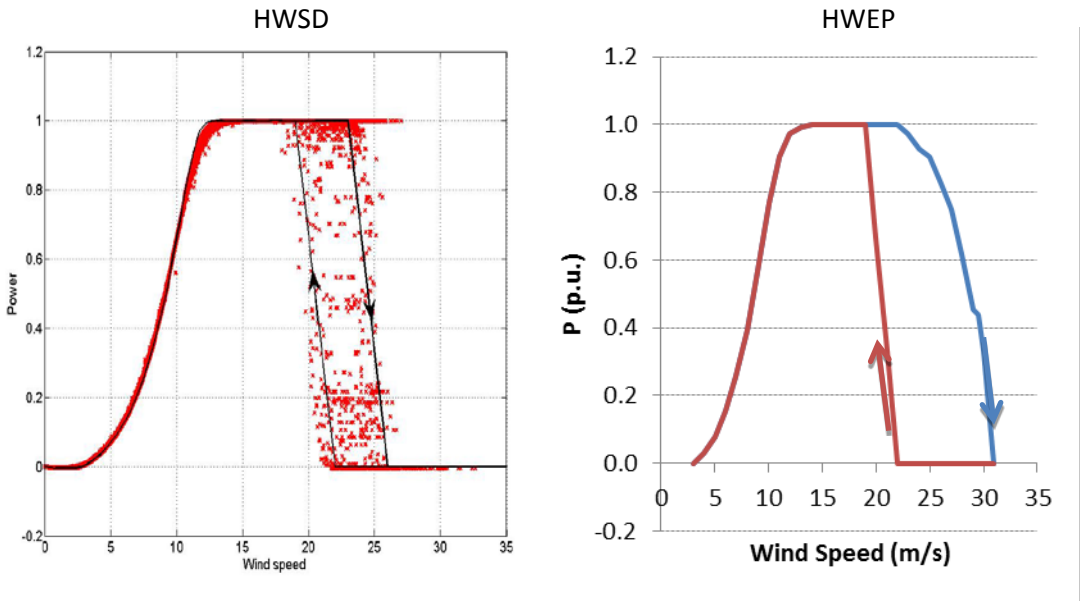


**Figure 11** Estimation of the aggregated power curve for Horns Rev 2 using CorWind with the Wind2Power module implementing the HWSD and HWEP storm control algorithm.

As already mentioned, this power curve can be considered representative for a wind power plant that covers an area of roughly 5x5 km and has an installed capacity of a couple hundred megawatts. In our scenarios though, there are wind power plants that will have installed capacities far larger than that, going all the way up to 4 GW. Simulating such a large power plant with the power curve presented above, would lead to an overestimation of the variability. Therefore, using this power curve and simulations done with CorWind, a number of aggregated power curves, for wind power plants up to 8 GW were calculated. The power curves are shown in Figure 12, while a zoom on the upper part of the power curves is shown in Figure 13, where the arrow indicates increasing wind power plant size.

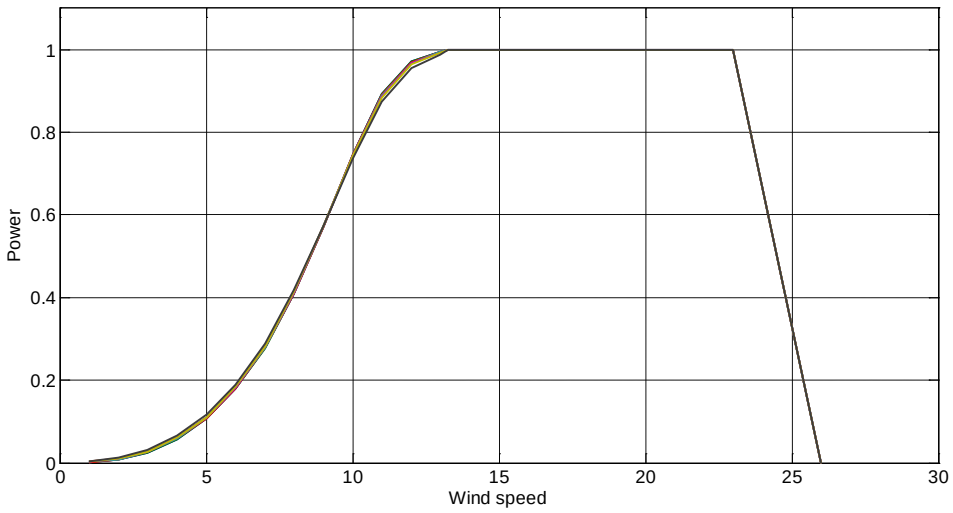


**Figure 12** Aggregated power curves

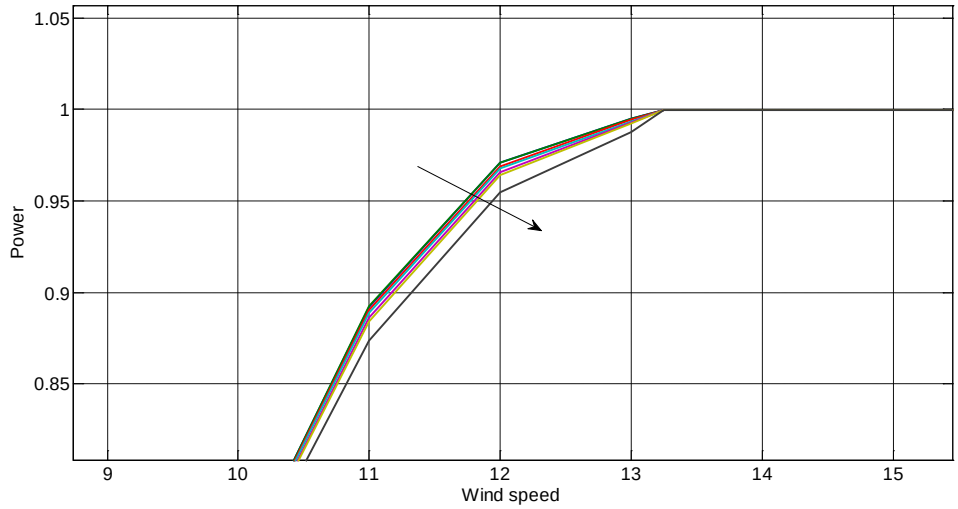


**Figure 13** Detail of the aggregated power curves; arrow indicates increasing wind power plant size

This is a note on the use of power curves in simulating wind power that has realistic variability. As per industry definition [17], power curves give the relationship between the 10minute power output and the wind speed averages. The relationship between the power output of a turbine given a wind speed given for 1second window is not available. We nevertheless use the same power curve to estimate the turbines power output given the wind speed time series with resolution that is less than 10minutes. This will introduce some discrepancy or even bias in the simulated power output. This is evident in Figure 10, where the simulated farm production is underestimated during most of the storm duration. This also partly explains the discrepancy in shutdown times between measurements and simulations, as shown in Figure 9. This is one of the limitations of the Wind2Power module inside CorWind.

## 2.2. Definitions

***Ramp rates***

The ramping is defined as the change in the mean value from a period to another:

$$P_{\text{ramp}}(n) = P_{\text{mean}}(n+1) - P_{\text{mean}}(n)$$

or graphically, in Figure 14.

The ramp rates are used as a measure of the variability induced by wind power and they represent the effort that the system needs to make in order to balance a system with varying wind power. In the definition used, negative values mean that there is decreasing wind power production, resulting in an increase of the production from other sources, i.e. conventional power plants.

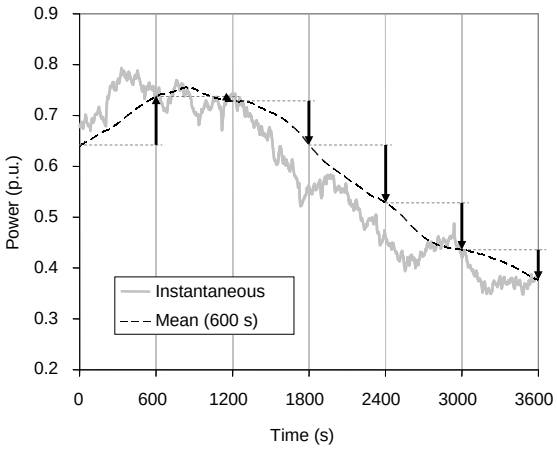


**Figure 14** Definition of ramping

***Maximum ramping***

The definition of maximum ramping applied in this report is quite similar to the definition of regulation applied in [5] and used in [6]. The intention is to define a quantity which can be used to assess if the frequency stability is threatened due to sudden (or short term) loss of wind power generation.

In order to quantify the short-term loss of wind power generation, the maximum ramping is defined as the difference between the present power and the minimum instantaneous power in the following time window $T_{win}$. Since the reserves must be allocated in advance, the positive reserve requirement is defined as the difference between the initial mean value and the minimum value in the next period. It has also been chosen to use a mean value of the present power rather than an instantaneous value with average periods $T_{ave}$ , because the initial value is rather random. The assessment of maximum ramp rates is involving a statistical window time $T_{win}$, which reflects the time scale of interest. The time scales of interest will depend on the power system size, load behavior and specific requirements to response times of reserves in the system. In order to study the wind variability in different time scales, the analysis is performed for several time windows. In this analysis, the time scale of interest is 15 minutes, meaning that in the rest of the report, when maximum ramping is used, **$T_{win}$ = 15 minutes.**

This definition of maximum ramping is illustrated for time windows $T_{win}$ = 60 min and average periods $T_{ave}$ = 15 min in Figure 15. The simulated (or measured) instantaneous power is shown in gray tone. The mean values for the latest 15 min are calculated and shown in black. For each 15 minute period, the reserve requirement is calculated as indicated by the arrows.

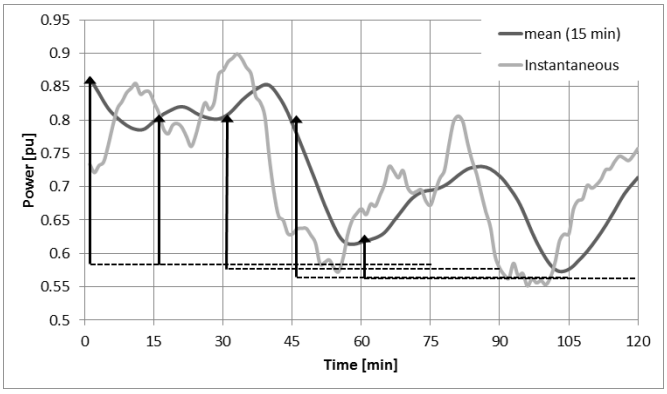


**Figure 15** Definition of maximum ramping

$$P_{\text{res}}(n) = P_{\text{mean}}\left[t(n) - T_{ave}\,; t(n)\right] - P_{\min}\left[t(n); t\,(n) + T_{win}\right]$$

Here, $[t_{\text{beg}}\,;\, t_{\text{end}}]$ denotes the time period from $t_{\text{beg}}$ to $t_{\text{end}}$. Note that with this definition, positive ramping means decreasing wind power that requires positive ramping from other power plants.

# 3. Reduction of offshore wind power forecast errors

## 3.1. Expected outcomes of this analysis

The following KPI as defined in [2] will be assessed in this chapter:

| | |
|---|---|
| KPI.16.TF2.1 | Reduction in ”worst case” forecast errors in the European power system by 2020 and 2030 with new storm control compared to old storm control [MW]. |

## 3.2. Main findings of demo 4

The analysis done in Demo 4 with regard to the performance of forecasting systems in detecting when shut-downs due to high wind speed will occur concluded that the ability of correctly forecasting storm events is quite poor for a wind farm with traditional High Wind Shut Down (HWSD) controllers in the wind turbines. An example of that is shown in Figure 16, where the forecasted vs the measured wind speed, for Horns Rev 2 wind farm is shown. The resulting wind power production forecast, updated every hour, compared to the measured one, is shown in Figure 17. It is easily observed that using the forecast for predicting wind farm shut-down due to high wind speed is not very reliable [3].

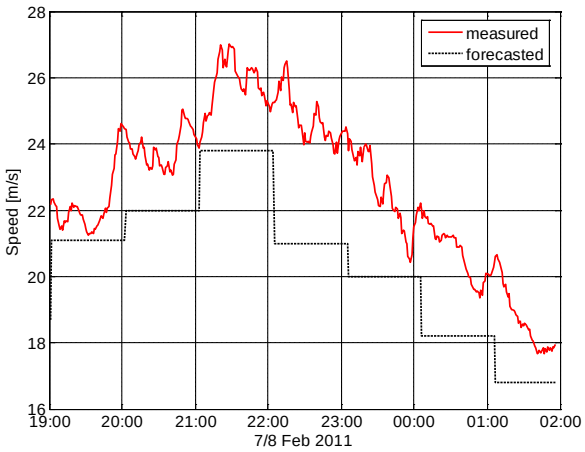


**Figure 16** 1-min measured vs forecasted wind speed

Once the High Wind Ride Through™ (HWRT™) was installed in all wind turbines in HR2, the wind power forecast performances improved significantly. As presented in detail in [4], the improvement is more than 50%, expressed as percentage of the installed capacities. The forecast error statistics, for all the recorded events, are given Table 3.1.

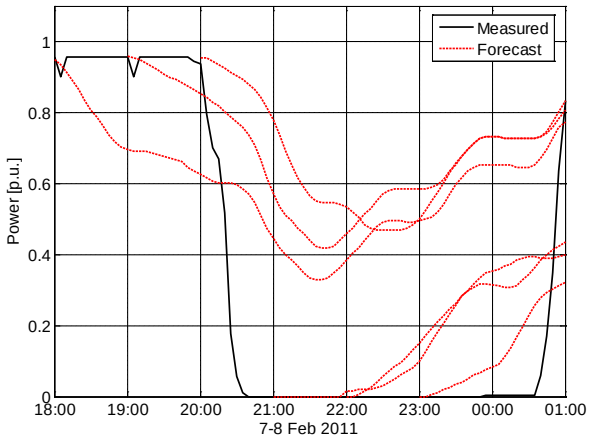


**Figure 17** Measured versus hourly intra-day forecast wind power

**Table 3.1** Forecast error statistics

| Event | Controller | Max forecast error [p.u.] | Average forecast error [p.u.] | Difference [p.u.] |
|---|---|---|---|---|
| 11-Nov-10 | HWSD | 0.80 | 0.77 | 0.51 |
| 12-Nov-10 | HWSD | 0.80 | | |
| 07-Feb-11 | HWSD | 0.72 | | |
| 24-Sep-12 | HWEP | 0.26 | 0.26 | |
| 14-Dec-12 | HWEP | 0.18 | | |
| 30-Jan-13 | HWEP | 0.35 | | |

## 3.3. Description of the assessment methodology and problem setting

The scope of this analysis is to quantify the reduction in the offshore wind power forecast error 2020 and 2030, provided that conventional HWSD storm controllers are replaced by High Wind Extended Production (HWEP) storm controllers performing similar to the SIEMENS HWRT™ controller. In the Demo 4 activities, the available and forecasted wind power used for this analysis – limited to Horns Rev 2 wind farm – were the ones used in the operation by Energinet.dk, the Danish TSO. The results presented in Table 3.1 are based on the online forecasts, updated every hour. In this report, the analysis is done for the entire North Europe and for a large number of future offshore wind farms, hence it was not possible to use any real available and forecasted wind power time series. The solution adopted was to use simulated wind power time series as described in chapter 2, and estimate the forecasted wind power time series using persistence. This is a conservative approach because modern forecast systems are usually better than persistence. The persistence estimated forecast is considered to be updated every hour – similar to the ones used by Energinet.dk – and for the hour the wind power is forecasted to have the same value as in the beginning of the hour. The forecast are created with this method for each synchronous area and for each meteorological year used in the simulations. As an example, the wind speed forecasts for a meteorological year is converted to wind power forecasts for each of the offshore wind farm projects in the

continental area for the year 2020. For this example, the sum of the forecasted wind power is shown in Figure 18.

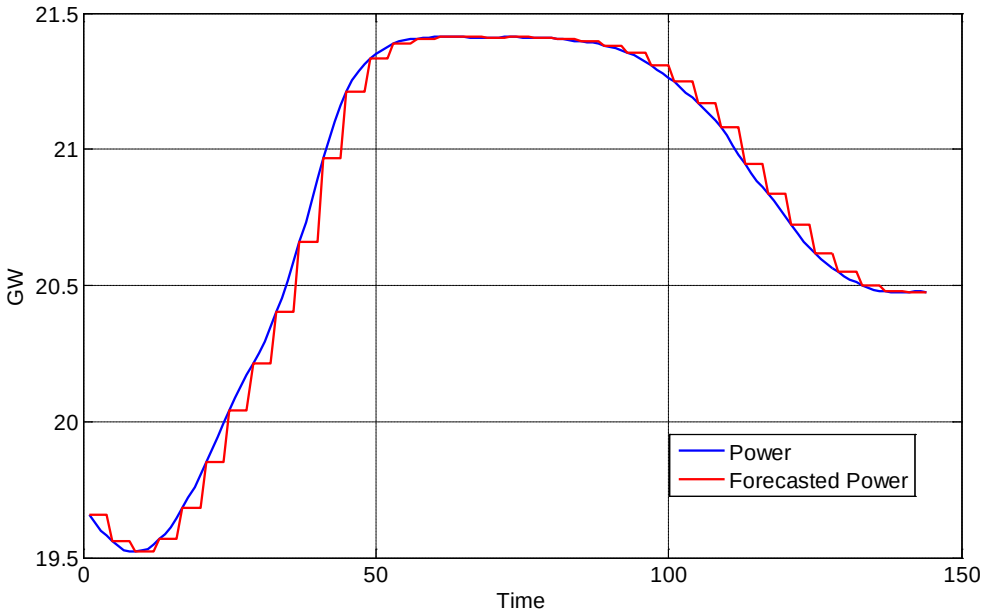


**Figure 18** Forecasted wind power for Continental area

### 3.4. Results

The error is quantified for each synchronous area, both for HWSD and HWEP. Since the forecast error is usually maximum during storm events, with wind power production going from full to zero with the HWSD controller, what is of interest here is to quantify the maximum forecast error for each year and each controller. The results are shown in Table 3.2, with the error quantified as percentage of the installed capacity, and in Table 3.3 with the error expressed in GW.

**Table 3.2** Forecast error for each controller, in 2020 (% of installed capacity)

| Meteo Year | Continental | | Nordic | | GB | | Ireland | |
|---|---|---|---|---|---|---|---|---|
| | HWSD | HWEP | HWSD | HWEP | HWSD | HWEP | HWSD | HWEP |
| **1** | 10.94% | 10.91% | 11.03% | 10.27% | 10.66% | 10.61% | 20.75% | 18.47% |
| **2** | 13.70% | 13.31% | 9.59% | 9.10% | 13.15% | 10.31% | 28.52% | 18.45% |
| **3** | 25.40% | 12.83% | 14.46% | 14.12% | 19.56% | 13.50% | 28.93% | 27.00% |
| **4** | 14.88% | 11.77% | 14.07% | 14.25% | 11.75% | 11.77% | 28.60% | 23.48% |
| **5** | 15.93% | 15.92% | 12.54% | 12.61% | 13.91% | 11.08% | 41.90% | 24.36% |
| **6** | 14.37% | 14.48% | 11.78% | 10.47% | 9.43% | 9.38% | 55.77% | 25.10% |
| **7** | 13.02% | 13.02% | 13.27% | 12.31% | 13.53% | 13.60% | 24.88% | 24.84% |
| **8** | 12.40% | 12.53% | 12.10% | 11.55% | 12.06% | 11.98% | 39.87% | 17.79% |
| **Average** | **15.08%** | **13.10%** | **12.36%** | **11.83%** | **13.01%** | **11.53%** | **33.65%** | **22.44%** |

**Table 3.3** Forecast error for each controller, in 2020 (GW)

| Meteo Year | Continental | | Nordic | | GB | | Ireland | |
|---|---|---|---|---|---|---|---|---|
| | HWSD | HWEP | HWSD | HWEP | HWSD | HWEP | HWSD | HWEP |
| **1** | 2.34 | 2.34 | 0.54 | 0.51 | 1.46 | 1.45 | 0.29 | 0.26 |
| **2** | 2.94 | 2.85 | 0.47 | 0.45 | 1.80 | 1.41 | 0.40 | 0.26 |
| **3** | 5.44 | 2.75 | 0.71 | 0.70 | 2.68 | 1.85 | 0.41 | 0.38 |
| **4** | 3.19 | 2.52 | 0.69 | 0.70 | 1.61 | 1.61 | 0.41 | 0.33 |
| **5** | 3.41 | 3.41 | 0.62 | 0.62 | 1.91 | 1.52 | 0.59 | 0.35 |
| **6** | 3.08 | 3.10 | 0.58 | 0.52 | 1.29 | 1.29 | 0.79 | 0.36 |
| **7** | 2.79 | 2.79 | 0.65 | 0.61 | 1.86 | 1.87 | 0.35 | 0.35 |
| **8** | 2.66 | 2.68 | 0.60 | 0.57 | 1.65 | 1.64 | 0.57 | 0.25 |
| **Average** | **3.23** | **2.81** | **0.61** | **0.58** | **1.78** | **1.58** | **0.48** | **0.32** |

In order to have a sense of the improvement (or not) in the maximum forecast error, Table 3.4 shows the ration between the maximum forecast errors, i.e. $FE_{HWEP}/FE_{HWSD}$. This gives an expression of the reduction of the forecast error, expressed as percentage of the initial forecast error. The results show that the forecast error has decreased for all areas, with significant reductions for Ireland and moderate for the rest of the systems.

**Table 3.4** Maximum forecast error difference per synchronous areas, in 2020

| Meteo Year | Continental | Nordic | GB | Ireland |
|---|---|---|---|---|
| **1** | 0.22% | 6.91% | 0.53% | 11.00% |
| **2** | 2.85% | 5.14% | 21.57% | 35.29% |
| **3** | 49.49% | 2.36% | 30.98% | 6.68% |
| **4** | 20.89% | -1.23% | -0.10% | 17.90% |
| **5** | 0.08% | -0.56% | 20.34% | 41.85% |
| **6** | -0.72% | 11.11% | 0.50% | 55.00% |
| **7** | 0.01% | 7.27% | -0.51% | 0.14% |
| **8** | -1.06% | 4.58% | 0.62% | 55.37% |
| **Average** | **8.97%** | **4.45%** | **9.24%** | **27.91%** |

The same results, for 2030, are shown in the following.

The forecast errors, for 2030, are shown in Table 3.5, with the error quantified as percentage of the installed capacity, and in Table 3.6 with the error expressed in GW.

**Table 3.5** Forecast error for each controller, in 2030 (% of installed capacity)

| Meteo Year | Continental | | Nordic | | GB | | Ireland | |
|---|---|---|---|---|---|---|---|---|
| | HWSD | HWEP | HWSD | HWEP | HWSD | HWEP | HWSD | HWEP |
| **1** | 10.73% | 10.91% | 9.09% | 10.27% | 13.66% | 10.61% | 24.76% | 18.47% |
| **2** | 12.18% | 13.31% | 5.11% | 9.10% | 12.91% | 10.31% | 34.78% | 18.45% |

| | | | | | | | | |
|---|---|---|---|---|---|---|---|---|
| **3** | 23.88% | 12.83% | 8.83% | 14.12% | 18.72% | 13.50% | 27.99% | 27.00% |
| **4** | 11.51% | 11.77% | 7.70% | 14.25% | 13.39% | 11.77% | 29.10% | 23.48% |
| **5** | 13.97% | 15.92% | 7.09% | 12.61% | 13.62% | 11.08% | 49.99% | 24.36% |
| **6** | 14.68% | 14.48% | 6.97% | 10.47% | 12.30% | 9.38% | 46.36% | 25.10% |
| **7** | 11.79% | 13.02% | 8.61% | 12.31% | 16.90% | 13.60% | 20.41% | 24.84% |
| **8** | 11.93% | 12.53% | 6.27% | 11.55% | 13.05% | 11.98% | 35.21% | 17.79% |
| **Average** | **13.83%** | **13.10%** | **7.46%** | **11.83%** | **14.32%** | **11.53%** | **33.57%** | **22.44%** |

**Table 3.6** Forecast error for each controller, in 2030 (GW)

| Meteo Year | Continental | | Nordic | | GB | | Ireland | |
|---|---|---|---|---|---|---|---|---|
| | HWSD | HWEP | HWSD | HWEP | HWSD | HWEP | HWSD | HWEP |
| **1** | 5.78 | 5.83 | 1.33 | 1.29 | 4.59 | 4.59 | 0.80 | 0.57 |
| **2** | 6.56 | 6.44 | 0.75 | 0.73 | 4.34 | 3.58 | 1.12 | 0.81 |
| **3** | 12.87 | 7.21 | 1.29 | 1.32 | 6.29 | 4.52 | 0.90 | 0.89 |
| **4** | 6.20 | 5.97 | 1.13 | 1.08 | 4.50 | 4.51 | 0.94 | 0.66 |
| **5** | 7.53 | 7.44 | 1.04 | 0.99 | 4.58 | 4.56 | 1.61 | 0.69 |
| **6** | 7.91 | 7.96 | 1.02 | 0.98 | 4.13 | 3.97 | 1.49 | 0.72 |
| **7** | 6.35 | 6.37 | 1.26 | 1.23 | 5.68 | 5.69 | 0.66 | 0.65 |
| **8** | 6.43 | 6.39 | 0.92 | 0.90 | 4.38 | 4.38 | 1.13 | 0.56 |
| **Average** | **7.46** | **6.70** | **1.09** | **1.06** | **4.81** | **4.47** | **1.08** | **0.69** |

Table 3.7 shows the ration between the maximum forecast errors for 2030. The results show that the forecast error has decreased for all areas, but with values that are lower than the ones for 2020.

**Table 3.7** Maximum forecast error difference per synchronous areas, in 2030

| Meteo Year | Continental | Nordic | GB | Ireland |
|---|---|---|---|---|
| **1** | -0.90% | 3.42% | 0.05% | 28.17% |
| **2** | 1.86% | 3.04% | 17.47% | 27.74% |
| **3** | 44.01% | -2.11% | 28.19% | 1.50% |
| **4** | 3.77% | 4.70% | -0.29% | 29.09% |
| **5** | 1.10% | 5.18% | 0.43% | 57.09% |
| **6** | -0.55% | 3.72% | 3.79% | 51.96% |
| **7** | -0.29% | 2.65% | -0.17% | 0.30% |
| **8** | 0.64% | 2.46% | 0.17% | 50.18% |
| **Average** | **6.20%** | **2.88%** | **6.21%** | **30.75%** |

### 3.5. Conclusions

Implementing the new storm controller that prevents wind power plants from suddenly shutting-down due to high wind speeds will have an inherently benefic impact on the wind power forecast error. The analysis presented, based on a rough estimation of the forecast error based on persistence, shows that due to the smoother behaviour of the wind power plants with HWEP, the wind power forecast error decreases with values that are in the range of 10-25% of the installed capacity.

# 4. Reduction in need for spinning reserves

## 4.1. Expected outcomes of this analysis

The following KPI as defined in [2] will be assessed in this chapter:

| | |
|---|---|
| KPI.16.TF2.2 | Reduction in the need for spinning reserves in the European power system by 2020 and 2030 with new storm control compared to old storm control [MW * hours/year]. |

The frequency stability in a synchronous power system area relies on the availability of sufficient online frequency containment (also called spinning) reserves to handle unexpectedly lost generation in the first instance. In the Continental European synchronous area, the reference incident is defined as the loss of 3,000 MW generation [7]. The corresponding dimensioning outage is 1,200 MW in the Nordic Synchronous area [8]. For GB and Ireland, the values considered in this report are 1,800 and 500 MW respectively.

In the second instance, the frequency containment reserves must be replaced by frequency replacement reserves, so that normal security level is re-established within a certain time. This reserve replacement usually takes up to 15 minutes, and additional loss of generation within this time period can cause frequency stability problems.

Normally, the need for frequency containment reserves is set so that the frequency remains stable after loss of the largest generation unit. However, the frequency stability can also be threatened if the wind power generation drops with more than the online frequency containment reserves within 15 minutes. This is normally not an issue because the total wind power changes relatively slow over large areas, but in case of a storm passage with massive scale offshore wind power concentrated in relatively small areas, the wind power generation can drop significantly within 15 minutes.

## 4.2. Results

### 4.2.1. Ramp Rates

The duration curves of the 15 min ramping for the four synchronous areas considered are shown in Figure 19 up to Figure 22. For each synchronous area, the ramp rates from all the simulated years were used. The target year is 2020, so the corresponding installed capacities were used. According to the definition of ramping, negative values mean decreasing wind power, hence need for up-regulation from other power plants in the system. Therefore, the attention is on the negative part of the duration curve. For comparison, the blue line on represents the dimensioning fault for the considered synchronous area.

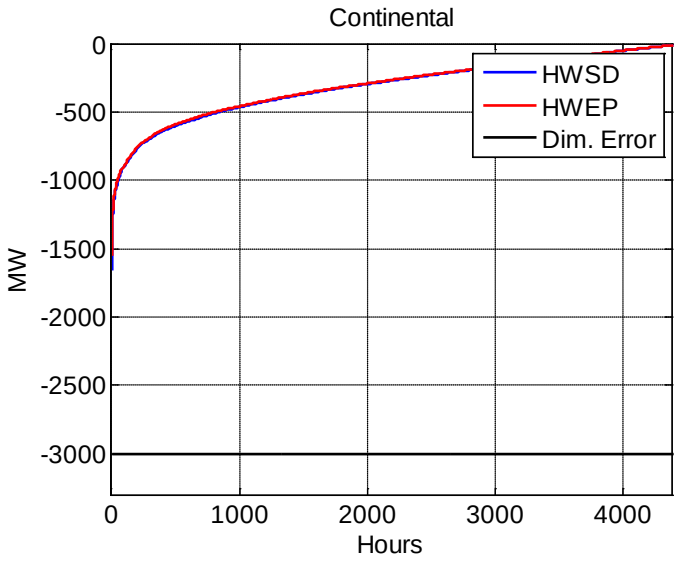


**Figure 19** Fifteen minute ramping duration curve for the Continental area in 2020

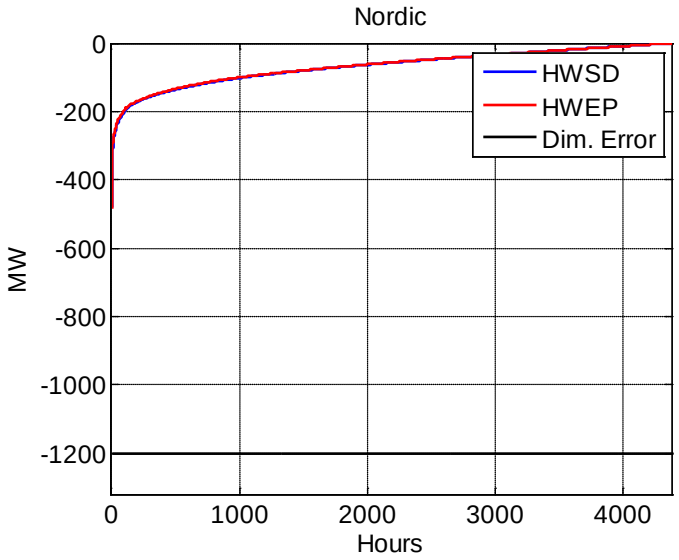


**Figure 20** Fifteen minute ramping duration curve for the Nordic area in 2020

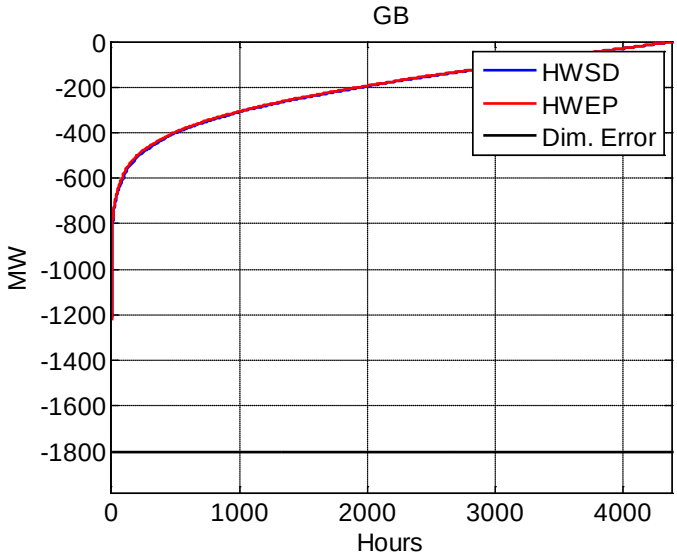


**Figure 21** Fifteen minute ramping duration curve for the GB area in 2020

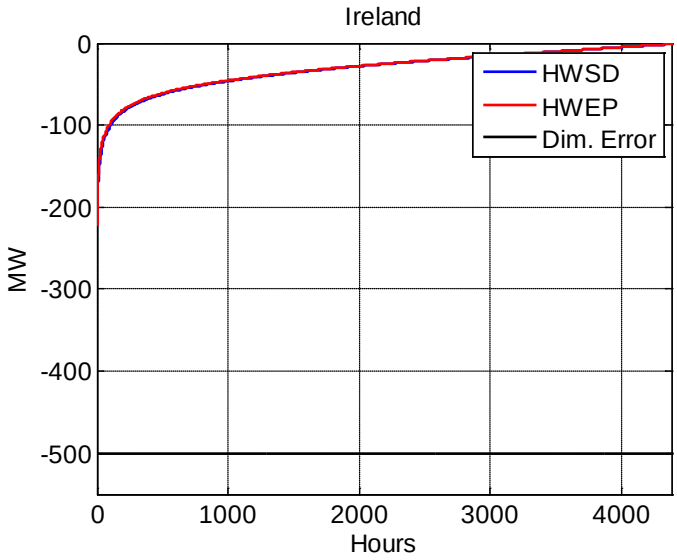


**Figure 22** Fifteen minute ramping duration curve for the island of Ireland area in 2020

**Table 4.1** Highest values of wind power ramping vs reference incident, 2020 scenario

| Synchronous Area | HWSD | HWEP | Reference incident |
|---|---|---|---|
| | MW | MW | MW |
| **Continental** | 1,661 | 1,548 | 3,000 |
| **Nordic** | 480 | 483 | 1,200 |
| **GB** | 1,212 | 1,222 | 1,800 |
| **Ireland** | 224 | 224 | 500 |

The first conclusion that can be drawn from the graphs is that for the 2020 scenario, wind power does not impose any threats to the secure operation of the power system in the

European synchronous areas. The maximum values of the 15 minutes ramping – for each controller – are given in Table 4.1. A direct observation deriving from that table is that the high wind speed events are not the ones behind the highest ramping; hence the difference between the two controllers is insignificant. This indicates that the normal operation variability is larger than the one due to the wind turbine behavior during storms, at least when looking at very large areas, such as the synchronous areas.

The results for 2030 are given in the following.

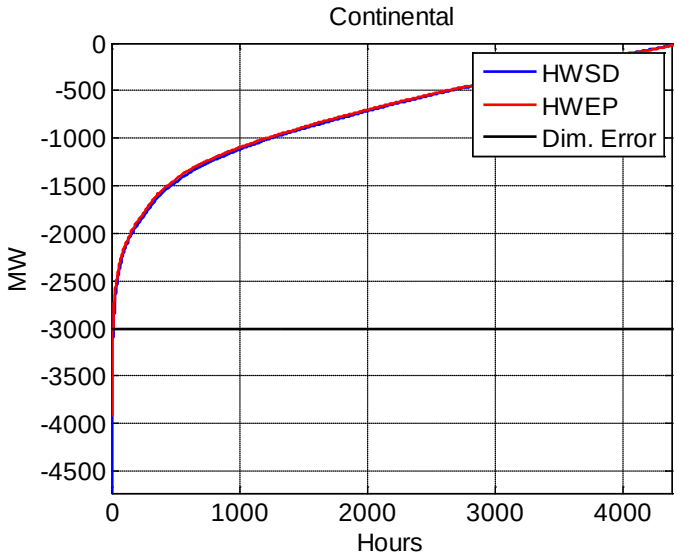


**Figure 23** Fifteen minute ramping duration curve for the Continental area in 2030

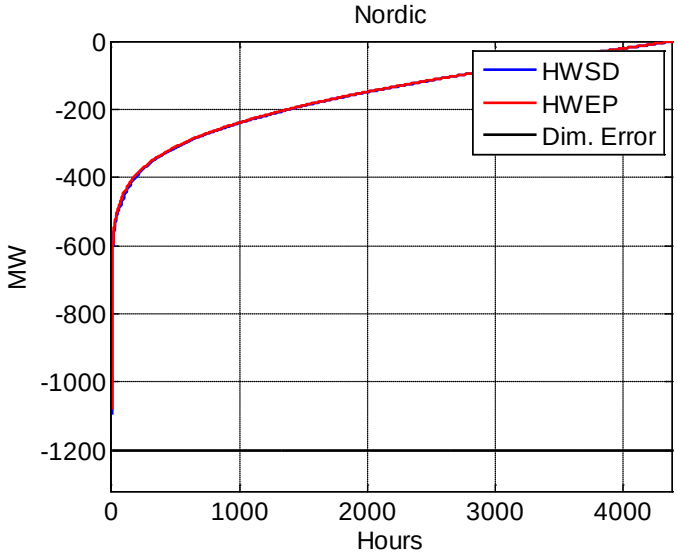


**Figure 24** Fifteen minute ramping duration curve for the Nordic area in 2030

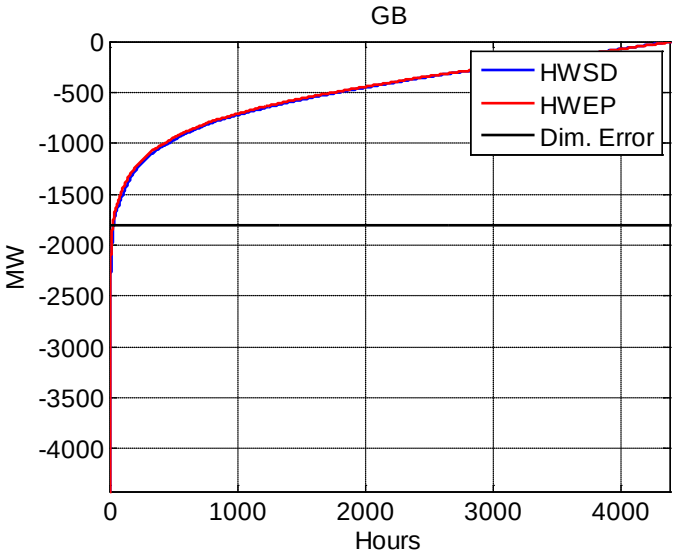


**Figure 25** Fifteen minute ramping duration curve for the GB area in 2030

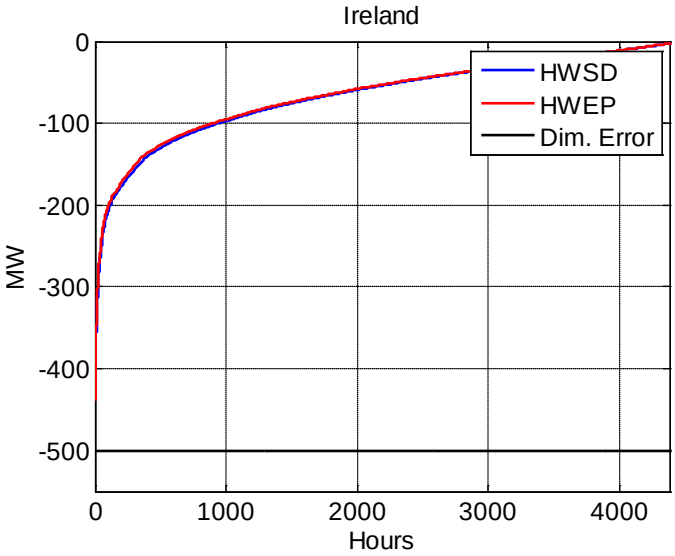


**Figure 26** Fifteen minute ramping duration curve for the Ireland area in 2030

When looking at the maximum values, for the 2030 scenario, one can notice that both Nordic and Irish synchronous systems seem to not be affected by the 15 min wind power ramping. On the other hand, Continental system and, especially, the GB system seem to be facing challenges, with the max value of the 15 min variability being significantly larger than the reference incidents, respectively, as it can be seen in Table 4.2. Another observation is that in the 2030 scenario, the highest value of the variability seems to be defined by an extreme wind event. The difference of the max ramping is significant in the Continental case, with more than 800 MW difference.

**Table 4.2** Highest values of wind power ramping vs reference incident, 2030 scenario

| Synchronous Area | HWSD | HWEP | Reference incident |
|---|---|---|---|

| | MW | MW | MW |
|---|---|---|---|
| **Continental** | 4,729 | 3,933 | 3,000 |
| **Nordic** | 1096 | 1082 | 1,200 |
| **GB** | 4,418 | 4,440 | 1,800 |
| **Ireland** | 439 | 438 | 500 |

For the Continental and GB systems, the ramping duration curves are zoomed into the hours when their values are exceeding the reference incident. One can notice that there is a number of around 10-12 and 25-30 hours that the system security is challenged by the offshore wind power variability, as shown in Figure 27 and Figure 28, respectively.

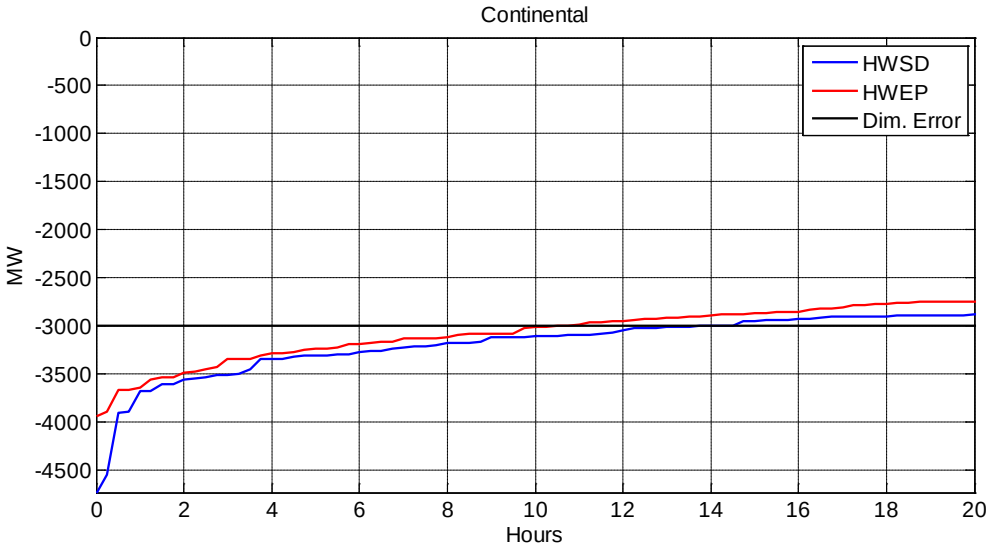


**Figure 27** Hours when ramping exceeds reference incident, Continental system, 2030

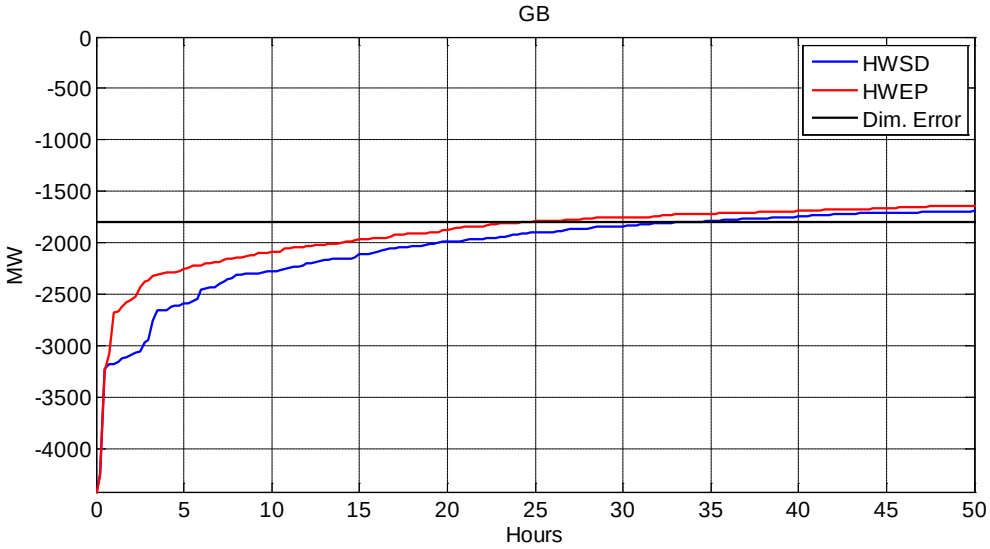


**Figure 28** Hours when ramping exceeds reference incident, GB system, 2030

### 4.2.2. Maximum ramping

The maximum ramping, is giving an image of the required spinning reserve – of course not detailed, as this would depend on a number of other parameters besides wind power production. In the following, the results of the maximum ramping for each synchronous area for 2020 and 2030 are given.

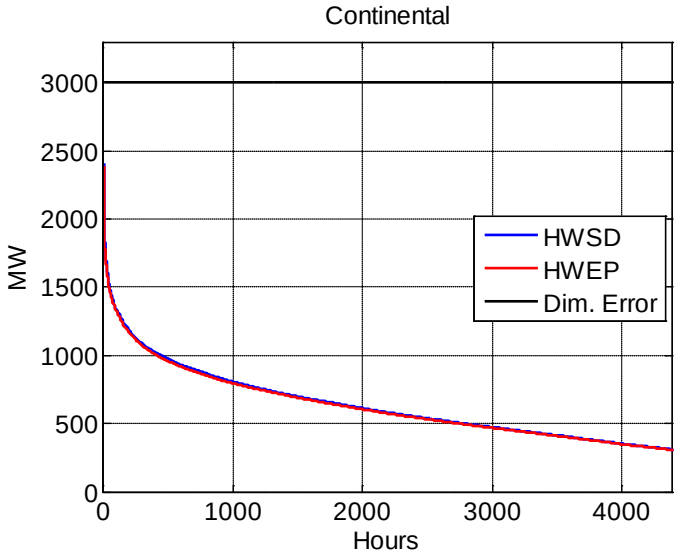


**Figure 29** Fifteen minutes maximum ramping duration curve for the Continental area in 2020

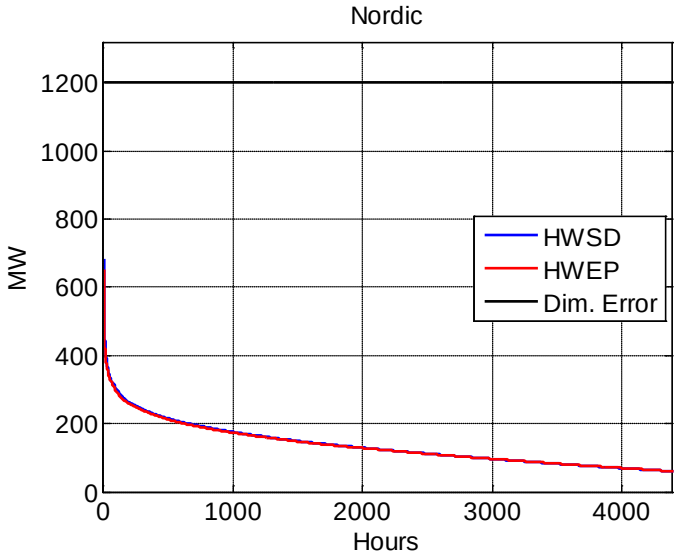


**Figure 30** Fifteen minute maximum ramping duration curve for the Nordic area in 2020

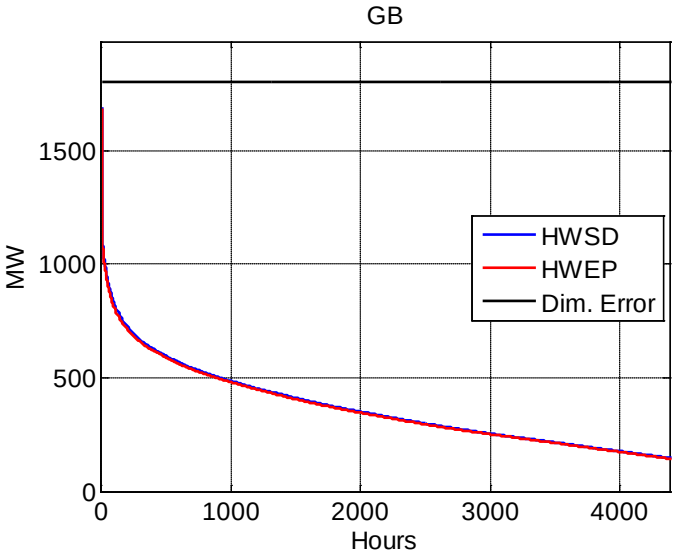


**Figure 31** Fifteen minute maximum ramping duration curve for the GB area in 2020

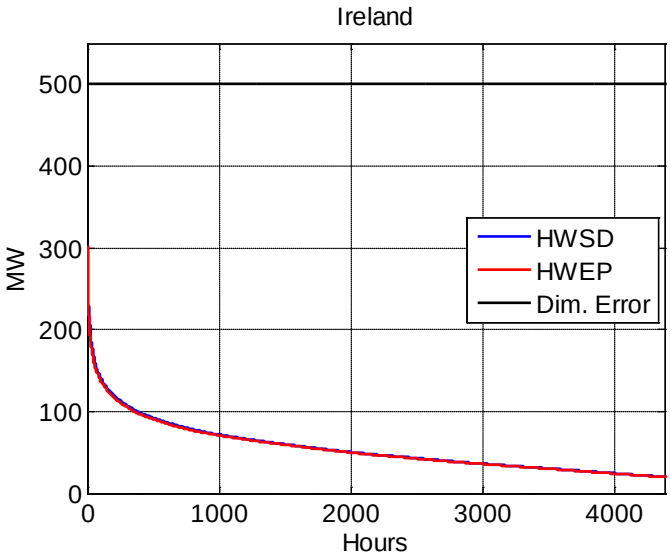


**Figure 32** Fifteen minute maximum ramping duration curve for the Irish system in 2020

**Table 4.3** Highest value of maximum ramping value vs reference incident, 2020 scenario

| Synchronous Area | HWSD | HWEP | Reference incident |
|---|---|---|---|
| | MW | MW | MW |
| **Continental** | 2,413 | 2,391 | 3,000 |
| **Nordic** | 684 | 652 | 1,200 |
| **GB** | 1,691 | 1,687 | 1,800 |

| | | | |
|---|---|---|---|
| **Ireland** | 302 | 302 | 500 |

With the 2020 scenario, offshore wind power maximum ramping does not exceed the reference incident value. Both Continental and GB systems though can experience values of wind power maximum ramping that are rather close to the reference incident values.

The results for the 2030 scenario are given in the following

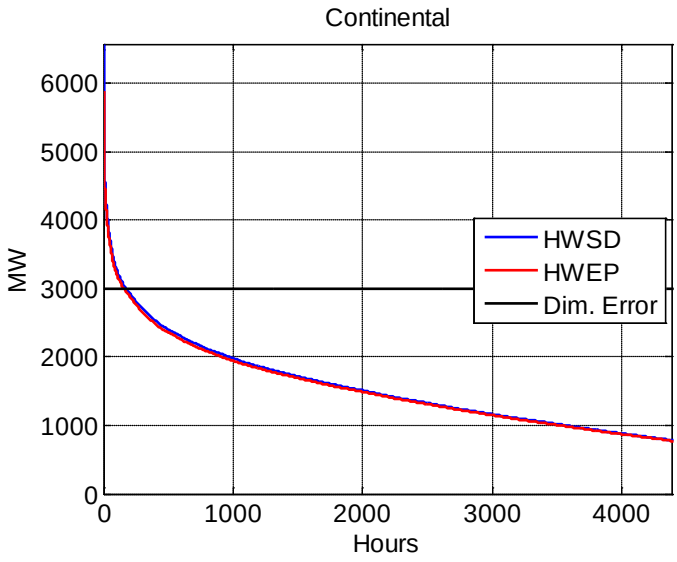


**Figure 33** Fifteen minute maximum ramping duration curve for the Continental area in 2030

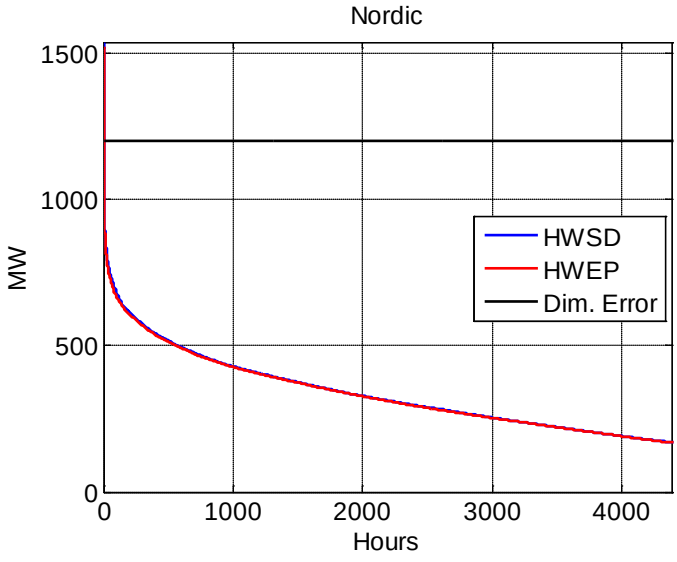


**Figure 34** Fifteen minute maximum ramping duration curve for the Nordic area in 2030

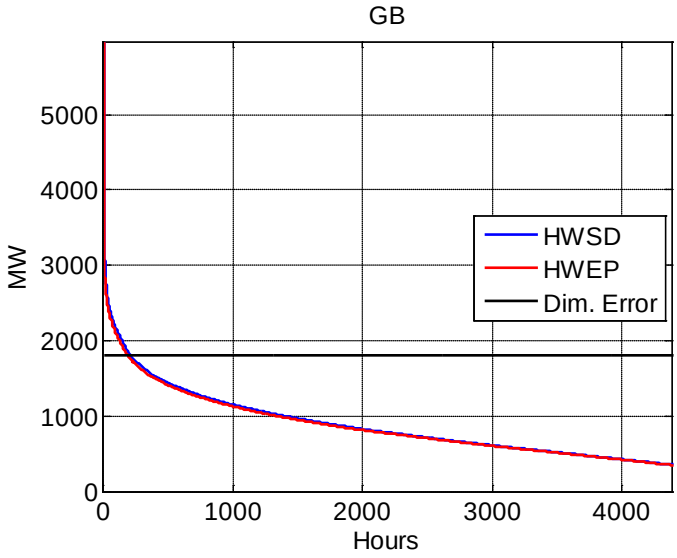


**Figure 35** Fifteen minute maximum ramping duration curve for the GB area in 2030

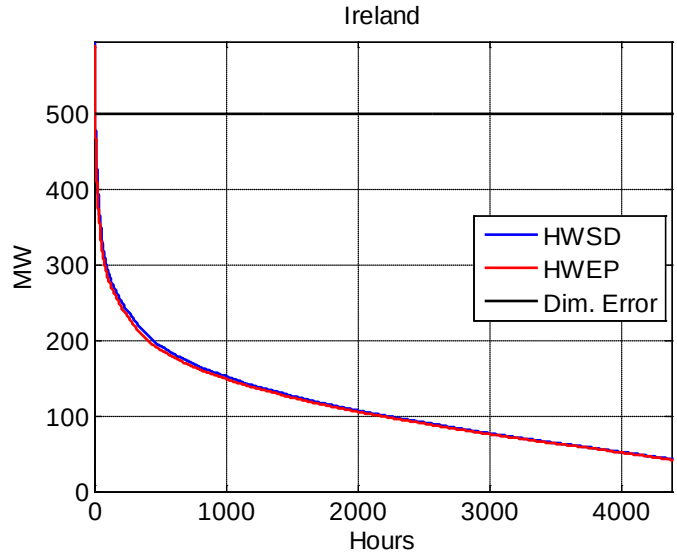


**Figure 36** Fifteen minute maximum ramping duration curve for the Irish system in 2030

**Table 4.4** Highest value of maximum ramping value vs reference incident, 2030 scenario

| Synchronous Area | HWSD | HWEP | Reference incident |
|---|---|---|---|
| | MW | MW | MW |
| **Continental** | 6,571 | 5,874 | 3,000 |
| **Nordic** | 1540 | 1525 | 1,200 |
| **GB** | 5,972 | 5,992 | 1,800 |
| **Ireland** | 595 | 591 | 500 |

For the 2030 scenario, the highest value of the maximum ramping is exceeding the reference incident for all areas considered, with the values of Continental and GB systems being more than double that. The number of hours when the maximum ramping is exceeding the reference incident can be seen in Figure 37 and Figure 42, for the Continental and GB system, respectively. For the Nordic and Irish system the number of hours is very small.

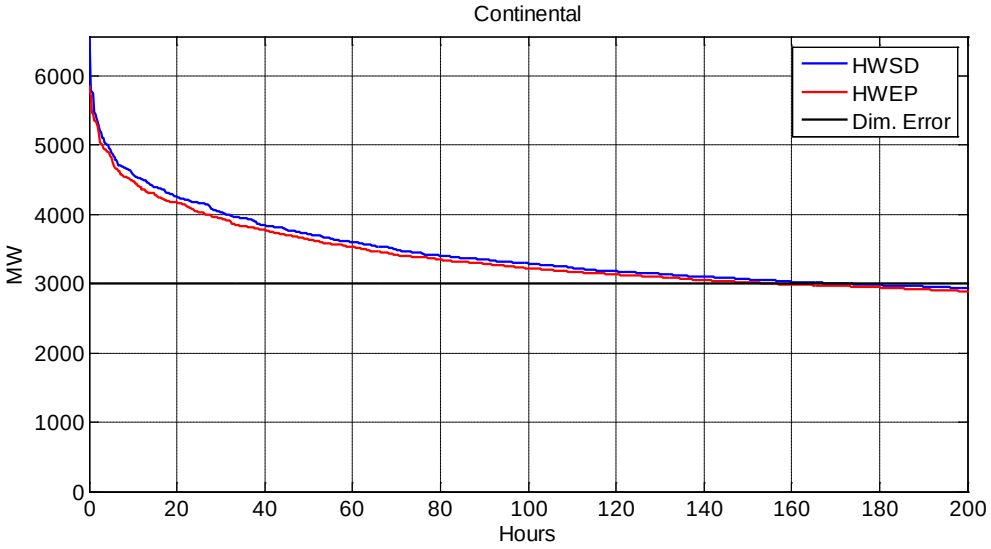


**Figure 37** Hours when max ramping exceeds reference incident, Continental system, 2030

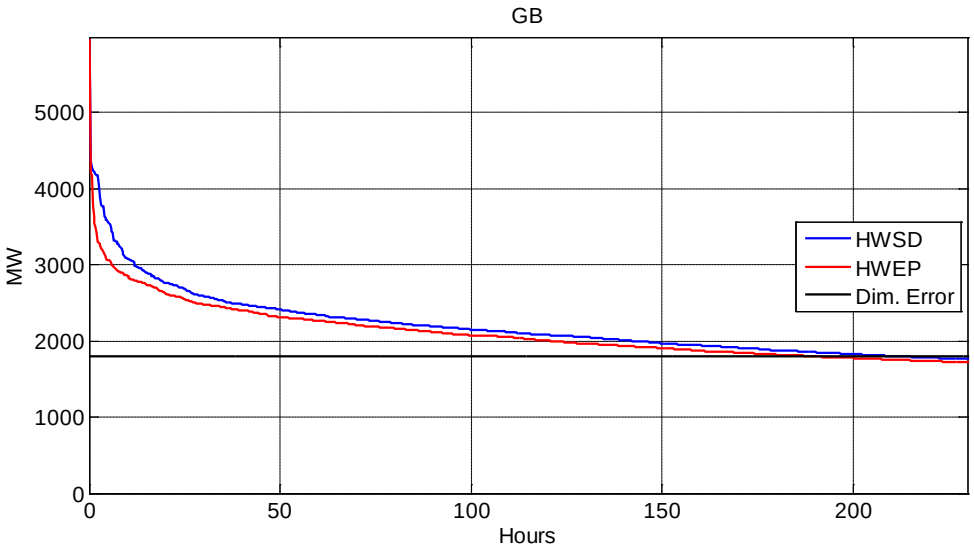


**Figure 38** Hours when max ramping exceeds reference incident, GB system, 2030

In order to see how the storm control impacts the wind power maximum ramping, the duration curve of the difference between HWSD and HWEP is plotted.

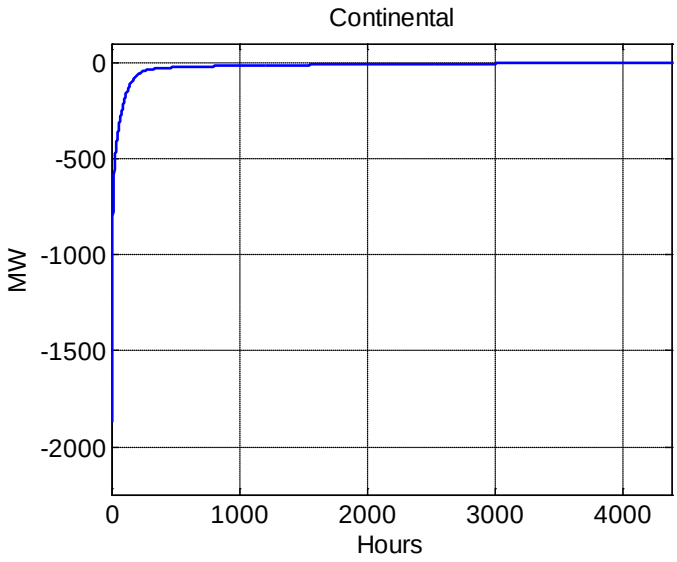


**Figure 39** Reduction in maximum ramping due to HWEP by 2020, Continental area

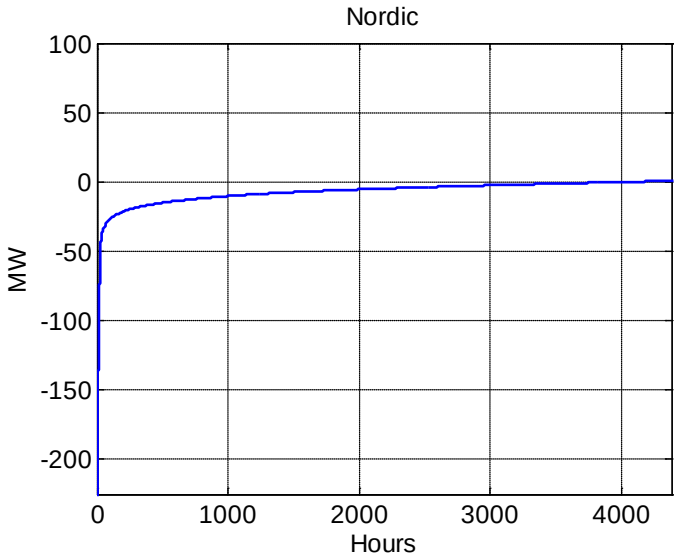


**Figure 40** Reduction in maximum ramping due to HWEP by 2020, Nordic area

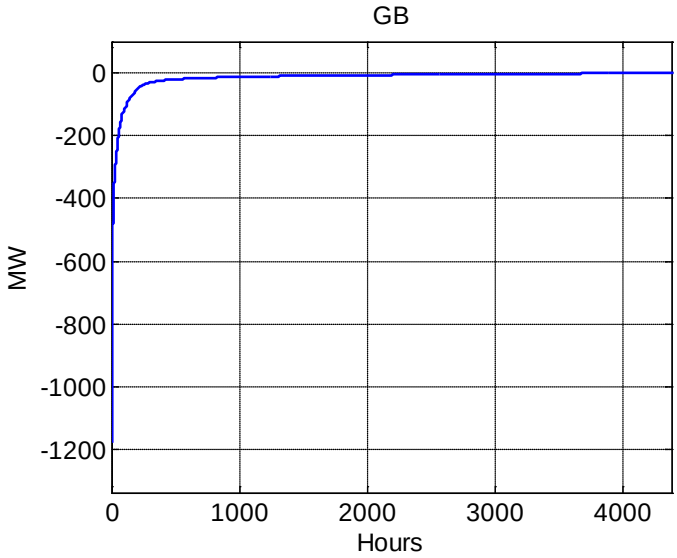


**Figure 41** Reduction in maximum ramping due to HWEP by 2020, GB area

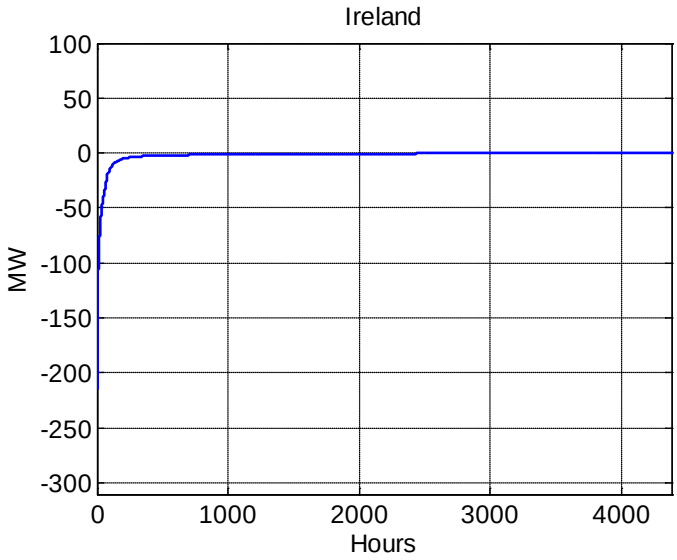


**Figure 42** Reduction in maximum ramping due to HWEP by 2020, Irish area

The reduction in the energy needed to cover wind power ramping down, i.e. negative values in the duration curve are quantified in Table 4.5 and is expressed in GWh for the whole period considered in the simulations and in percentage of the energy needed when HWSD is operating. The results indicate that by the use of HWEP, a reduction of the energy needed to cover wind power ramping down is between 1.5 and 6% for the areas considered.

**Table 4.5** Reduction of ramping energy by 2020 due to HWEP

| Synchronous Area | Ramp reduction | |
|---|---|---|
| | GWh | % of HWSD |
| **Continental** | 1264.45 | 5.70% |
| **Nordic** | 73.93 | 1.53% |

| | | |
|---|---|---|
| **GB** | 253.87 | 1.74% |
| **Ireland** | 69.25 | 3.08% |

The same results for 2030 are given in the following.

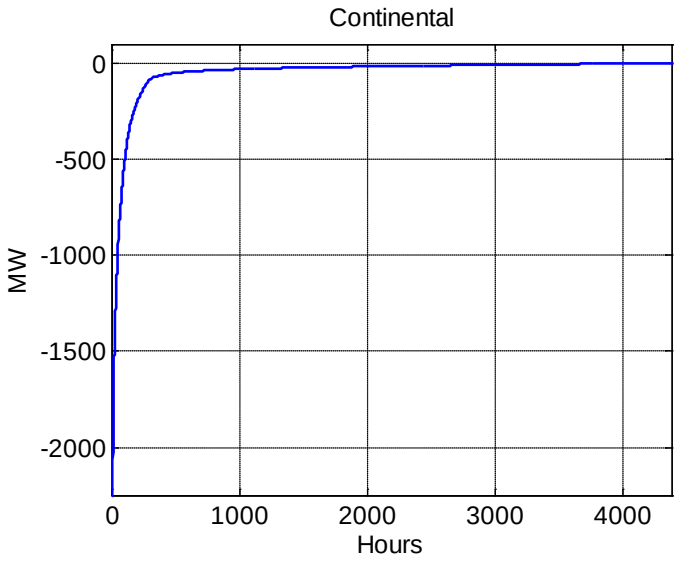


**Figure 43** Reduction in maximum ramping due to HWEP by 2030, Continental area

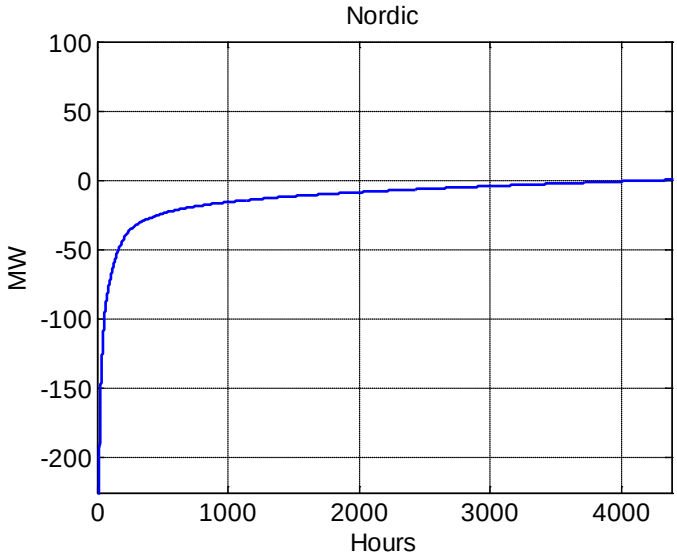


**Figure 44** Reduction in maximum ramping due to HWEP by 2030, Nordic area

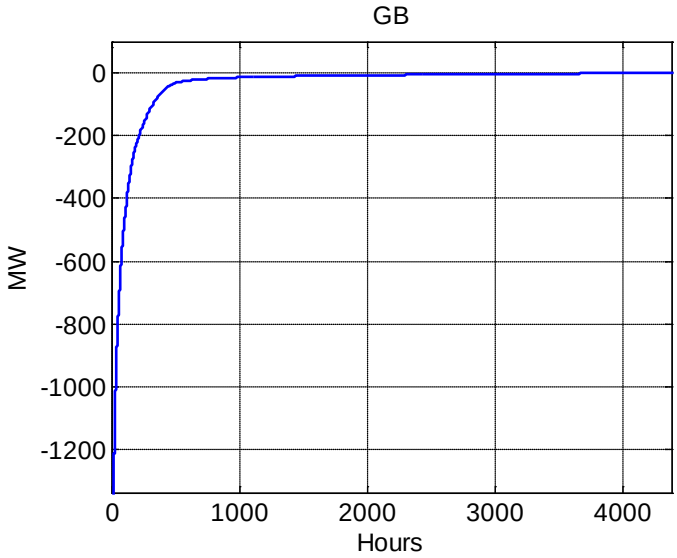


**Figure 45** Reduction in maximum ramping due to HWEP by 2030, GB area

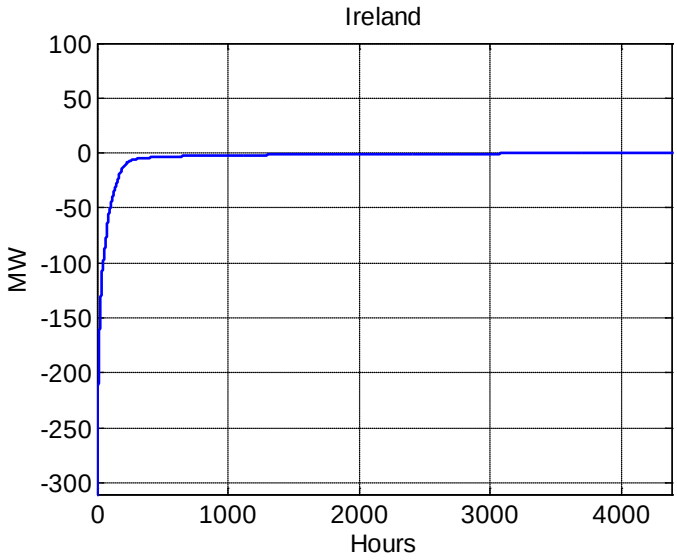


**Figure 46** Reduction in maximum ramping due to HWEP by 2030, Irish area

For the 2030 scenario, the reduction in the energy needed for balancing the wind power maximum ramping is significant, ranging from 10 to more than 50% for the areas considered. The exact values are given in Table 4.6.

**Table 4.6** 4.7 Reduction of ramping energy by 2030 due to HWEP

| Synchronous Area | Ramp reduction | |
|---|---|---|
| | GWh | % of HWSD |
| **Continental** | 3818.74 | 28.20% |
| **Nordic** | 1402.20 | 55.24% |
| **GB** | 1369.52 | 10.82% |

| | | |
|---|---|---|
| **Ireland** | 891.59 | 46.89% |

### 4.3. Conclusions

Analysing the variability of wind power in the four synchronous systems considered revealed that, for 2020, wind power maximum ramping – while significant at times – it does reach values higher than the current dimensioning incidents values. For the 2030 scenario, this is not the case, with the values exceeding – for some systems significantly – the dimensioning incidents values. This indicates that the offshore wind power variability should be considered in frequency stability assessment. This work has not been analysing how this should be done, but one way could be to introduce a variable requirement for frequency containment reserves, depending on the current wind power production.

In terms of spinning reserves due to wind power variability, the new storm controller

# 5. Impact on offshore wind power generation

## 5.1. Expected outcomes of this analysis

| | |
|---|---|
| KPI.16.TF2.3 | Increased wind power production with the new storm control compared to the old storm control |

## 5.2. Main findings of demo 4 (Energinet.dk)

In order to assess the difference in the energy produced during the events, the energy production with both controllers was calculated. It can be seen from Table 3 that between 403 and 1120MWh is gained by installing the HWRT™ controller compared to the old HWSD controller. During a year we only expect a few (less than 10) number of storms. At the location where the turbines are located it is expected that 1MW of installed capacity will produce about 4300MWh during one year. This means that the HR2 wind farm will produce about 0.9TWh during a year. The result of introducing the HWRT™ controller is an increase of production during storm events although the increase in the total yearly production is insignificant.

**Table 5.1** Energy production during the recorded events

| Event | Energy [MWh] | | |
|---|---|---|---|
| | HWSD | HWRT | Difference [MWh] |
| 11-11-2010 | 656 | 1194 | 537 |
| 12-11-2010 | 600 | 1003 | 403 |
| 07-02-2011 | 886 | 1556 | 671 |
| 24-09-2012 | 1391 | 2296 | 905 |
| 14-12-2012 | 3680 | 4186 | 506 |
| 30-01-2013 | 1390 | 2510 | 1120 |

## 5.3. Results

The total energy production, for both HWSD and HWEP, was calculated, per synchronous area, and compared. The results should be read as indicative, as the exact AEP will depend on several other factors than just the storm controller.

In Table 5.2, the total energy production for the Continental synchronous area and for each controller, together with the difference, expressed in TWh and in percentage of the base case, is given. The average increase in the energy production is a little over 1.5 TWh or around 1.71% of the base case (HWSD) annual energy production. The same total production can be expressed in terms of Equivalent Full Load Hours (EFLH), defined as the ratio between the produced energy and the maximum possible energy, multiplied by the number of hours in a year:

$$\text{EFLH} = \frac{\text{Produced Energy}}{\text{Maximum Possible Energy}} * \text{Hours}$$

**Table 5.2** AEP for Continental synchronous area in 2020

| Year | HWSD | HWEP | Diff | Percentage |
|---|---|---|---|---|
| | TWh | TWh | TWh | % |
| **1** | 92.45 | 93.83 | 1.38 | 1.47% |
| **2** | 95.50 | 97.18 | 1.68 | 1.73% |
| **3** | 99.24 | 101.23 | 1.99 | 1.96% |
| **4** | 102.59 | 104.34 | 1.75 | 1.68% |
| **5** | 95.38 | 96.85 | 1.47 | 1.52% |
| **6** | 87.18 | 88.78 | 1.60 | 1.80% |
| **7** | 100.69 | 102.48 | 1.79 | 1.75% |
| **8** | 98.25 | 99.99 | 1.73 | 1.73% |
| **Average** | **96.41** | **98.09** | **1.67** | **1.71%** |

The EFHP for the Continental synchronous area, in 2020, are given in Table 5.3.

**Table 5.3** EFLH for Continental synchronous area in 2020

| Year | HWSD | HWEP | Diff | Percentage |
|---|---|---|---|---|
| | Hours | Hours | Hours | % |
| **1** | 4314 | 4378 | 64 | 1.47% |
| **2** | 4456 | 4534 | 78 | 1.73% |
| **3** | 4630 | 4723 | 93 | 1.96% |
| **4** | 4787 | 4869 | 82 | 1.68% |
| **5** | 4450 | 4519 | 69 | 1.52% |
| **6** | 4068 | 4142 | 74 | 1.80% |
| **7** | 4698 | 4782 | 84 | 1.75% |
| **8** | 4584 | 4665 | 81 | 1.73% |
| **Average** | **4451** | **4526** | **78** | **1.71%** |

In Table 5.4, the total energy production for the Nordic synchronous area and for each controller, together with the difference, expressed in TWh and in percentage of the base case, is given. The average increase in the energy production is a little over 0.03 TWh or around 0.15% of the base case (HWSD) annual energy production. The EFLH are given in

**Table 5.4** AEP for Nordic synchronous area in 2020

| Year | HWSD | HWEP | Diff | Percentage |
|---|---|---|---|---|
| | TWh | TWh | TWh | % |
| **1** | 16.94 | 16.95 | 0.01 | 0.07% |
| **2** | 18.41 | 18.47 | 0.06 | 0.33% |
| **3** | 19.72 | 19.76 | 0.04 | 0.21% |
| **4** | 18.93 | 18.94 | 0.01 | 0.06% |

| | | | | |
|---|---|---|---|---|
| **5** | 17.87 | 17.88 | 0.02 | 0.10% |
| **6** | 16.67 | 16.68 | 0.00 | 0.02% |
| **7** | 19.83 | 19.88 | 0.05 | 0.26% |
| **8** | 19.05 | 19.08 | 0.03 | 0.17% |
| **Average** | **18.43** | **18.46** | **0.03** | **0.15%** |

**Table 5.5** EFLH for Nordic synchronous area in 2020

| Year | HWSD | HWEP | Diff | Percentage |
|---|---|---|---|---|
| | Hours | Hours | Hours | % |
| **1** | 3447 | 3450 | 2 | 0.07% |
| **2** | 3747 | 3759 | 12 | 0.33% |
| **3** | 4014 | 4022 | 8 | 0.21% |
| **4** | 3852 | 3855 | 2 | 0.06% |
| **5** | 3637 | 3640 | 4 | 0.10% |
| **6** | 3394 | 3394 | 1 | 0.02% |
| **7** | 4037 | 4047 | 10 | 0.26% |
| **8** | 3877 | 3884 | 7 | 0.17% |
| **Average** | **4451** | **4526** | **6** | **0.15%** |

In Table 5.6, the total energy production for the GB synchronous area and for each controller, together with the difference, expressed in TWh and in percentage of the base case, is given. The average increase in the energy production is a little below 1 TWh or around 1.5% of the base case (HWSD) annual energy production. The EFLH for the GB area in 2020 are given in Table 5.7

**Table 5.6** AEP for GB synchronous area in 2020

| Year | HWSD | HWEP | Diff | Percentage |
|---|---|---|---|---|
| | TWh | TWh | TWh | % |
| **1** | 59.98 | 60.71 | 0.73 | 1.20% |
| **2** | 62.83 | 63.83 | 1.00 | 1.56% |
| **3** | 60.74 | 61.86 | 1.12 | 1.81% |
| **4** | 66.52 | 67.48 | 0.96 | 1.42% |
| **5** | 60.24 | 61.06 | 0.82 | 1.35% |
| **6** | 52.99 | 53.86 | 0.87 | 1.62% |
| **7** | 64.17 | 65.05 | 0.88 | 1.36% |
| **8** | 60.76 | 61.75 | 0.99 | 1.60% |
| **Average** | **61.03** | **61.95** | **0.92** | **1.49%** |

**Table 5.7** EFLH for GB synchronous area in 2020

| Year | HWSD | HWEP | Diff | Percentage |
|---|---|---|---|---|

| | Hours | Hours | Hours | % |
|---|---|---|---|---|
| **1** | 4375 | 4428 | 53 | 1.20% |
| **2** | 4583 | 4655 | 73 | 1.56% |
| **3** | 4430 | 4512 | 82 | 1.81% |
| **4** | 4852 | 4922 | 70 | 1.42% |
| **5** | 4393 | 4453 | 60 | 1.35% |
| **6** | 3865 | 3929 | 64 | 1.62% |
| **7** | 4680 | 4744 | 64 | 1.36% |
| **8** | 4432 | 4504 | 72 | 1.60% |
| **Average** | **4451** | **4526** | **67** | **1.49%** |

In Table 5.8, the total energy production for the Irish synchronous area and for each controller, together with the difference, expressed in TWh and in percentage of the base case, is given. The average increase in the energy production is 0.02 TWh or around 0.35% of the base case (HWSD) annual energy production. The EFLH are given in Table 5.9

**Table 5.8** AEP for Irish synchronous area in 2020

| Year | HWSD | HWEP | Diff | Percentage |
|---|---|---|---|---|
| | TWh | TWh | TWh | % |
| **1** | 6.19 | 6.20 | 0.01 | 0.11% |
| **2** | 6.83 | 6.86 | 0.03 | 0.48% |
| **3** | 6.45 | 6.50 | 0.05 | 0.71% |
| **4** | 7.07 | 7.09 | 0.01 | 0.20% |
| **5** | 6.83 | 6.84 | 0.01 | 0.16% |
| **6** | 5.68 | 5.72 | 0.04 | 0.71% |
| **7** | 7.06 | 7.08 | 0.02 | 0.26% |
| **8** | 6.87 | 6.89 | 0.02 | 0.27% |
| **Average** | **6.62** | **6.65** | **0.02** | **0.36%** |

**Table 5.9** EFLH for Irish synchronous area in 2020

| Year | HWSD | HWEP | Diff | Percentage |
|---|---|---|---|---|
| | Hours | Hours | Hours | % |
| **1** | 4363 | 4368 | 5 | 0.11% |
| **2** | 4815 | 4838 | 23 | 0.48% |
| **3** | 4548 | 4580 | 33 | 0.71% |
| **4** | 4985 | 4995 | 10 | 0.20% |
| **5** | 4815 | 4823 | 8 | 0.16% |
| **6** | 4000 | 4029 | 29 | 0.71% |
| **7** | 4975 | 4988 | 13 | 0.26% |
| **8** | 4842 | 4855 | 13 | 0.27% |
| **Average** | **4451** | **4526** | **17** | **0.36%** |

The same results, for the 2030 scenario are given in the following.

**Table 5.10** AEP for Continental synchronous area in 2030

| Year | HWSD | HWEP | Diff | Percentage |
|---|---|---|---|---|
| | TWh | TWh | TWh | % |
| **1** | 235.51 | 238.51 | 3.00 | 1.26% |
| **2** | 246.31 | 250.12 | 3.81 | 1.52% |
| **3** | 254.87 | 259.45 | 4.58 | 1.77% |
| **4** | 263.53 | 267.59 | 4.06 | 1.52% |
| **5** | 244.91 | 248.12 | 3.21 | 1.29% |
| **6** | 224.84 | 228.28 | 3.44 | 1.51% |
| **7** | 258.95 | 263.07 | 4.12 | 1.57% |
| **8** | 251.92 | 255.72 | 3.80 | 1.49% |
| **Average** | **247.60** | **251.36** | **3.75** | **1.49%** |

**Table 5.11** EFLH for Continental synchronous area in 2030

| Year | HWSD | HWEP | Diff | Percentage |
|---|---|---|---|---|
| | Hours | Hours | Hours | % |
| **1** | 4346 | 4402 | 55 | 1.26% |
| **2** | 4546 | 4616 | 70 | 1.52% |
| **3** | 4703 | 4788 | 85 | 1.77% |
| **4** | 4863 | 4938 | 75 | 1.52% |
| **5** | 4520 | 4579 | 59 | 1.29% |
| **6** | 4149 | 4213 | 63 | 1.51% |
| **7** | 4779 | 4855 | 76 | 1.57% |
| **8** | 4649 | 4719 | 70 | 1.49% |
| **Average** | **4451** | **4526** | **69** | **1.49%** |

**Table 5.12** AEP for Nordic synchronous area in 2030

| Year | HWSD | HWEP | Diff | Percentage |
|---|---|---|---|---|
| | TWh | TWh | TWh | % |
| **1** | 52.70 | 52.78 | 0.08 | 0.15% |
| **2** | 58.16 | 58.41 | 0.24 | 0.42% |
| **3** | 59.30 | 59.53 | 0.23 | 0.38% |
| **4** | 57.01 | 57.18 | 0.18 | 0.31% |
| **5** | 54.26 | 54.39 | 0.13 | 0.24% |
| **6** | 50.84 | 50.90 | 0.05 | 0.11% |
| **7** | 60.86 | 61.08 | 0.22 | 0.37% |
| **8** | 57.12 | 57.32 | 0.19 | 0.34% |
| **Average** | **56.28** | **56.45** | **0.17** | **0.29%** |

**Table 5.13** EFLH for Nordic synchronous area in 2030

| Year | HWSD | HWEP | Diff | Percentage |
|---|---|---|---|---|
| | Hours | Hours | Hours | % |
| **1** | 3561 | 3566 | 5 | 0.15% |
| **2** | 3931 | 3947 | 16 | 0.42% |
| **3** | 4007 | 4023 | 15 | 0.38% |
| **4** | 3853 | 3864 | 12 | 0.31% |
| **5** | 3666 | 3675 | 9 | 0.24% |
| **6** | 3436 | 3440 | 4 | 0.11% |
| **7** | 4113 | 4128 | 15 | 0.37% |
| **8** | 3860 | 3873 | 13 | 0.34% |
| **Average** | **4451** | **4526** | **11** | **0.29%** |

**Table 5.14** AEP for GB synchronous area in 2030

| Year | HWSD | HWEP | Diff | Percentage |
|---|---|---|---|---|
| | TWh | TWh | TWh | % |
| **1** | 154.38 | 155.15 | 0.77 | 0.50% |
| **2** | 166.98 | 169.27 | 2.28 | 1.35% |
| **3** | 158.77 | 161.09 | 2.32 | 1.44% |
| **4** | 171.81 | 173.63 | 1.82 | 1.05% |
| **5** | 158.92 | 160.07 | 1.15 | 0.72% |
| **6** | 139.09 | 140.35 | 1.26 | 0.90% |
| **7** | 167.68 | 169.51 | 1.82 | 1.08% |
| **8** | 160.08 | 161.81 | 1.73 | 1.07% |
| **Average** | **159.71** | **161.36** | **1.65** | **1.01%** |

**Table 5.15** EFLH for GB synchronous area in 2030

| Year | HWSD | HWEP | Diff | Percentage |
|---|---|---|---|---|
| | Hours | Hours | Hours | % |
| **1** | 4594 | 4618 | 23 | 0.50% |
| **2** | 4970 | 5038 | 68 | 1.35% |
| **3** | 4725 | 4794 | 69 | 1.44% |
| **4** | 5113 | 5167 | 54 | 1.05% |
| **5** | 4730 | 4764 | 34 | 0.72% |
| **6** | 4139 | 4177 | 38 | 0.90% |
| **7** | 4990 | 5045 | 54 | 1.08% |
| **8** | 4764 | 4816 | 52 | 1.07% |
| **Average** | **4451** | **4526** | **49** | **1.01%** |

**Table 5.16** AEP for Irish synchronous area in 2030

| Year | HWSD | HWEP | Diff | Percentage |
|---|---|---|---|---|
| | TWh | TWh | TWh | % |
| **1** | 14.13 | 14.15 | 0.02 | 0.12% |
| **2** | 15.52 | 15.61 | 0.09 | 0.55% |
| **3** | 14.61 | 14.72 | 0.11 | 0.75% |
| **4** | 16.19 | 16.23 | 0.04 | 0.25% |
| **5** | 15.55 | 15.58 | 0.03 | 0.22% |
| **6** | 12.99 | 13.08 | 0.09 | 0.69% |
| **7** | 16.19 | 16.25 | 0.05 | 0.34% |
| **8** | 15.79 | 15.85 | 0.06 | 0.35% |
| **Average** | **15.12** | **15.18** | **0.06** | **0.41%** |

**Table 5.17** EFLH for Irish synchronous area in 2030

| Year | HWSD | HWEP | Diff | Percentage |
|---|---|---|---|---|
| | Hours | Hours | Hours | % |
| **1** | 3271 | 3276 | 4 | 0.12% |
| **2** | 3594 | 3614 | 20 | 0.55% |
| **3** | 3382 | 3407 | 26 | 0.75% |
| **4** | 3748 | 3758 | 9 | 0.25% |
| **5** | 3601 | 3608 | 8 | 0.22% |
| **6** | 3007 | 3028 | 21 | 0.69% |
| **7** | 3749 | 3762 | 13 | 0.34% |
| **8** | 3657 | 3670 | 13 | 0.35% |
| **Average** | **4451** | **4526** | **14** | **0.41%** |

The impact of the storm controller on the AEP increases with the installed capacity. This increase reverses for very large installed capacities, i.e. Continental and UK in 2030 have more than 50 and 30 GW installed capacity, respectively, where the extra production, expressed as percentage of the base case (HWSD controller), decreases. The values, per scenario and synchronous area, are given in Table 5.18.

**Table 5.18** Increased production due to HWEP, expressed as percentage of base case

| Synch. Area | 2020 | 2030 |
|---|---|---|
| **Continental** | 1.71% | 1.49% |
| **Nordic** | 0.15% | 0.29% |
| **UK** | 1.49% | 1.01% |
| **Ireland** | 0.36% | 0.41% |

## 5.4. Conclusions

The comparison of the wind energy production with the two controllers shows that the new controller increases the amount of energy produced. This is expected, since the new controller enables the wind power plants to produce at higher wind speeds. The increase in the amount of energy produced is directly proportional to the number of high wind speed events. For the years analysed in the report, the average increase in wind energy production was in the range of up to app. 2% of the annual production. The values should be read with care, since the exact numbers will depend on several other factors.

# 6. Impact of added hydro generation capacity with corresponding grid reinforcements

## 6.1. Expected outcomes of this analysis

| | |
|---|---|
| KPI.16.TF2.5 | Economic benefit in the European power system by 2020, utilizing the potential contribution of added HVDC connections and added Nordic hydro capacity, to the large-scale integration of wind power in northern Europe [Euro/year] |

## 6.2. Description of the assessment methodology and problem setting

The WILMAR (Wind Power Integration in Liberalised Electricity Markets) model (reference) consists of two modules: the Scenario Tree Tool (STT) and the Joint Market Model (JMM). The STT is a tool for generating scenario trees for wind and demand. The scenario trees are subsequently used by the JMM to find the hourly economic unit commitment and dispatch of electricity generation with respect to uncertainty in wind and demand. In this study, uncertainty is disregarded in the unit commitment and dispatch problem solution, and hence scenario trees are not needed for the JMM simulations. Therefore, only the JMM is used in this study.

The Joint Market Model (JMM) forms the economic dispatch of power generation, flows, and consumption given generation unit data, trading capacities, loads, fuel and emission prices, as well as, information on wind, hydro etc. JMM operates with a dynamic planning horizon of up to 36 hours and an hourly time resolution. JMM includes integrated optimisation of electricity storages over the planning horizon (up to 36 hours). This makes it possible to model e.g. cold storages and electric vehicles as described in [16]. Three modes are available: Perfect forecast, deterministic with forecast error, and stochastic. The three modes differ in the way stochasticity in wind and demand is treated. In this project JMM is run in perfect forecast mode, which assumes perfect information throughout the entire planning horizon.

Due to the nature of the wind forecasts used in this project, the hourly dispatch values can be interpreted as “Day-ahead” or “Spot-market” solution and serves as input to the SIMBA model.

## 6.3. Results

The WILMAR model was used to assess the effects on the N. European system of increasing hydropower and transmission capacity from Norway concurrently, based on the assumptions of perfect load and wind forecast. The scenarios considered in the simulations are the ones presented in [18]. The WILMAR results show that there are some non-negligible benefits borne out of this addition to the Norwegian system, as it leads to reduced costs for the N. European electricity system in general. The WILMAR runs also lead to the conclusion that upgrading the capacity of transmission systems is necessary for making use of the new hydro capacity.

The first result produced by WILMAR is the day-ahead average marginal prices over the whole year, showing the effect of the expansion of hydropower and transmission capacity. The original case is called the base case while the case including the hydropower and transmission upgrades is labeled as the ‘hydro case’. Results are depicted in Table 6.1 below.

**Table 6.1** System Marginal Price for Base and Hydro cases

| Region | System Average Marginal Price- Base Case (€/MWh) | System Average Marginal Price – Hydro Case (€/MWh) | Difference (€/MWh) |
|---|---|---|---|
| **Germany** | 38.27 | 38.00 | -0.27 |
| **Denmark, East** | 38.27 | 38.00 | -0.27 |
| **Denmark, West** | 33.14 | 33.87 | 0.73 |
| **Belgium** | 30.11 | 31.29 | 1.18 |
| **Finland** | 40.92 | 40.75 | -0.17 |
| **France** | 29.45 | 30.23 | 0.78 |
| **Netherlands** | 20.87 | 20.81 | -0.06 |
| **Norway** | 36.48 | 36.41 | -0.08 |
| **Poland** | 27.49 | 28.86 | 1.37 |
| **Sweden** | 33.78 | 33.86 | 0.09 |
| **UK** | 26.44 | 28.23 | 1.78 |

The results from table 1 show that the marginal price effect is ambiguous, with almost half the areas having their average marginal price increased while it decreased for the other half. This effect mostly stems from the fact that due to the introduction of new transmission and hydropower capacity in Norway, there is a redistribution of production among areas and the marginal units change for each area. As a result, the price effect does not lead to any concrete conclusions about the benefits of the capacity expansion and their magnitude.

Table 6.2 however shows a much more clear effect, as it depicts the costs of the N. European system for each included area in the simulation. As WILMAR is optimizing (minimizing) costs rather than prices, it makes sense that the magnitude and direction of any effect will be shown most prominently here.

**Table 6.2** Total System Costs for Base and Hydro cases

| Regions & Costs (M€) | $CO_2$ cost | $CO_2$ cost-Hydro | Fuel cost | Fuel cost-Hydro | OMV cost | OMV cost - Hydro | Total energy cost | Total energy cost - Hydro | Difference |
|---|---|---|---|---|---|---|---|---|---|
| **Germany** | 3672 | 3567 | 5682 | 5486 | 251 | 244 | 9605 | 9297 | - |

| | | | | | | | | | |
|---|---|---|---|---|---|---|---|---|---|
| | | | | | | | | | 308 |
| **DK West** | 118 | 119 | 225 | 229 | 13 | 13 | 356 | 361 | 5 |
| **DK East** | 94 | 96 | 147 | 150 | 7 | 7 | 248 | 253 | 5 |
| **Belgium** | 188 | 179 | 1320 | 1276 | 17 | 16 | 1526 | 1471 | -55 |
| **Finland** | 54 | 55 | 823 | 870 | 483 | 485 | 1360 | 1410 | 50 |
| **France** | 237 | 234 | 3604 | 3601 | 4614 | 4626 | 8456 | 8461 | 5 |
| **Netherlands** | 1270 | 1224 | 1725 | 1651 | 245 | 242 | 3240 | 3117 | -123 |
| **Norway** | 0 | 0 | 0 | 0 | 494 | 502 | 494 | 502 | 8 |
| **Poland** | 1723 | 1709 | 1551 | 1542 | 326 | 325 | 3600 | 3576 | -24 |
| **Sweden** | 68 | 67 | 913 | 1106 | 933 | 966 | 1914 | 2139 | 225 |
| **UK** | 1138 | 1066 | 3871 | 3629 | 708 | 717 | 5718 | 5412 | -306 |
| **Total** | 8562 | 8315 | 19862 | 19539 | 8091 | 8142 | 36515 | 35997 | -518 |

As it can be seen, the system costs change significantly, by approximately 518 mil. Euros, after the introduction of the new hydro and transmission capacity. Particularly, system costs are most reduced for the areas to which the interconnections' capacity increases (Germany, Netherlands, UK). However, the costs for the Nordic countries actually increases, as the new interconnections mean that existing plans work more and to higher capacity, increasing the operation and maintenance costs for Norway and particularly Sweden, due to the increased usage of hydro, nuclear and biomass in those two countries. However, from a European perspective, the changes are clearly positive; the cost reductions in continental Europe and the UK far outweigh the moderately increased costs in the Nordics.

The new fuel mix is shown in Figure 47, where a significant shift in the utilization of different fuels in electricity production can be noticed.

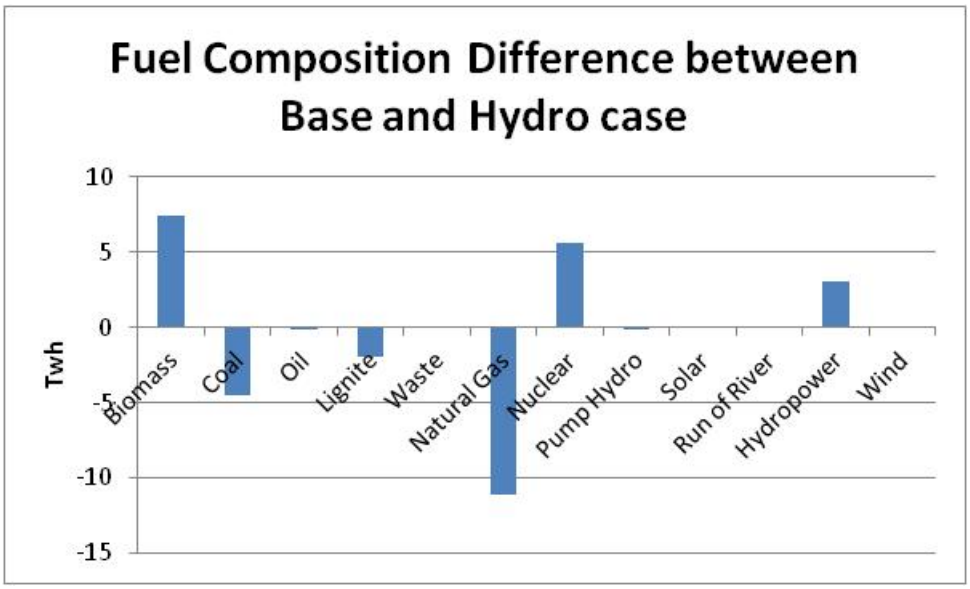


**Figure 47** Fuel usage difference between Base and Hydro cases

Figure 47 indicates that the changes are not mostly a result of increased Norwegian hydro capacity, but of the increased transmission capacity that allows Swedish & Finnish production as well to be transmitted in continental Europe in greater volumes. This is because it can be seen that the greatest changes are an increase in biomass and nuclear power utilization and a proportionate reduction in more conventional fossil fuel utilization, like coal, lignite and particularly natural gas. The origins of this displacement lie mostly in the Swedish system. To illustrate this point, the German, Norwegian and Swedish changes in the fuel composition of the production are produced in Figure 48 and Figure 49 below.

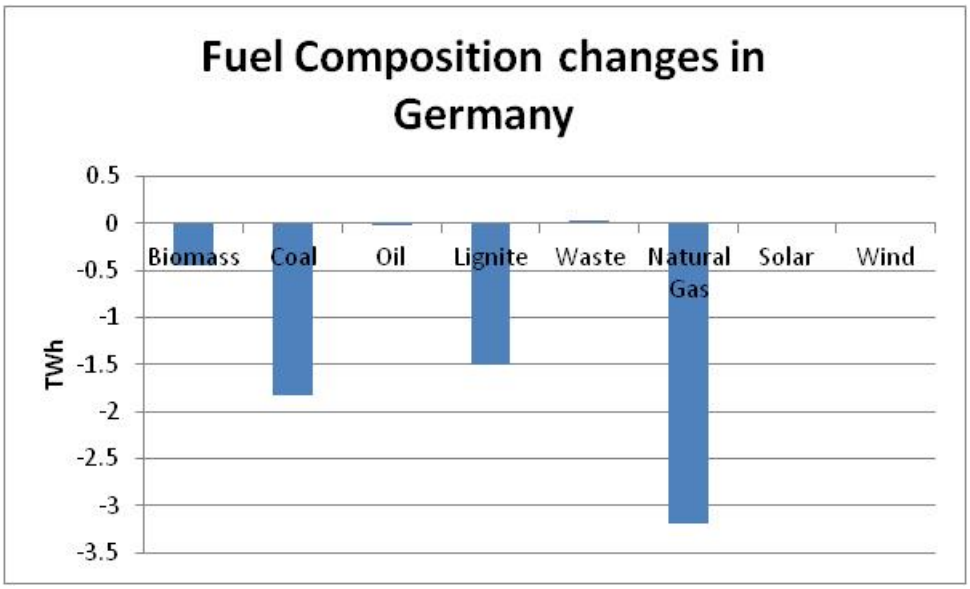


**Figure 48** Fuel Composition changes after Hydro case in Germany

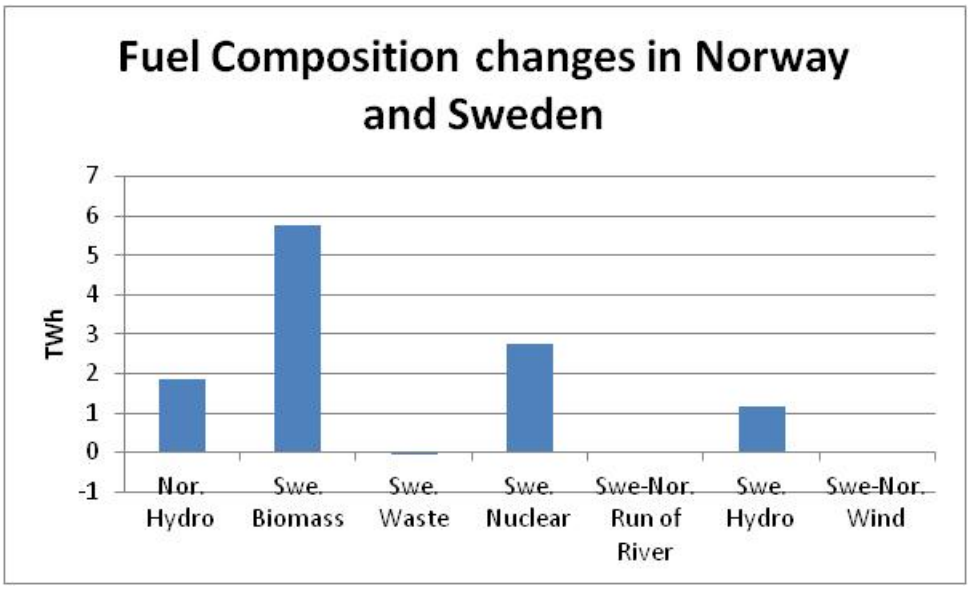


**Figure 49** Fuel Composition changes after Hydro case in Norway and Sweden

As it can be seen, German production is decreased throughout, while Norwegian and particularly Swedish production is increased. It is also apparent that the biggest changes occur in the utilization of Swedish biomass and nuclear power plants rather than in Norway itself, showing that it's not the hydropower capacity upgrade that is necessarily critical for these costs reductions. However, these results are entirely reliant on the projections for the capacity of different power plants in 2030 and would therefore change considerably if those projections were altered.

The displacement of natural gas, lignite and coal has the benefit of reducing the CO2 emissions throughout the N. European System, as more carbon-free nuclear and hydropower is utilized. With CO2 price assumed to be 25 €/ton and the CO2 costs presented above, it is straightforward to calculate the change in emissions after the introduction of the new hydropower and transmission capacity, shown in Figure 50 below.

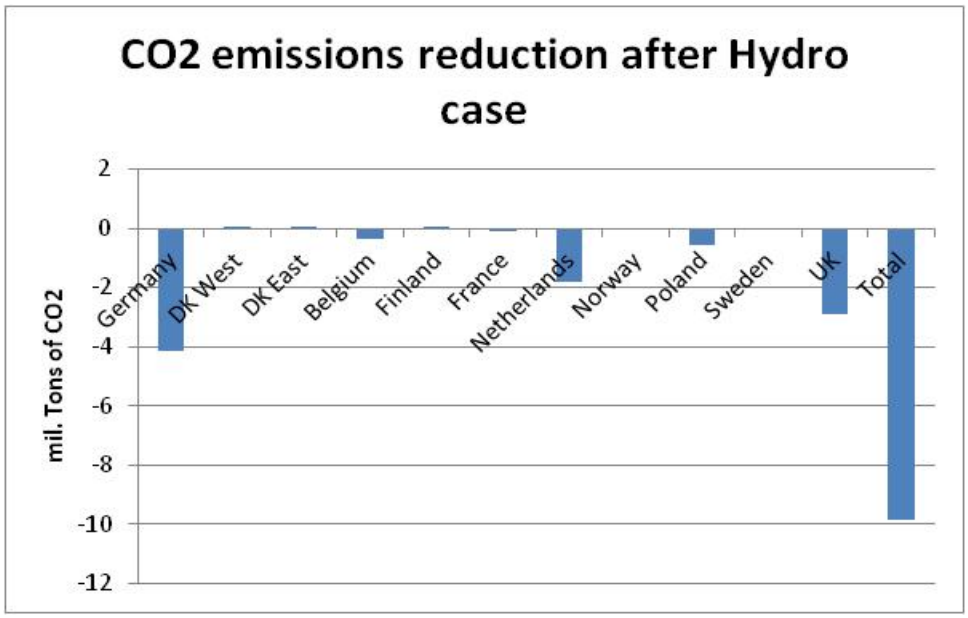


**Figure 50** Change in $CO_2$ emissions, Hydro-Base case, mil. tons

Similar to costs, CO2 emissions have decreased most prominently for the countries whose production has decreased most due to the upgrades in hydropower and transmission capacity. This has not been accompanied by an increase in CO2 emissions in the Nordic countries, as production there is either carbon-free (hydropower, nuclear) or almost so (biomass). The overall result is a clear reduction in emissions, to the effect of 10 million tons. However, this is based on a CO2 price of 25 €/ton which is a level quite removed from today's prices and their current projections.

The final benefit of the increase in hydropower and transmission capacity is the possibility to avoid wind shedding. Indeed, results that are summarized in Figure 51 do indicate that wind shedding is reduced substantially, by a total of 1.75 TWh across the entire N. European system.

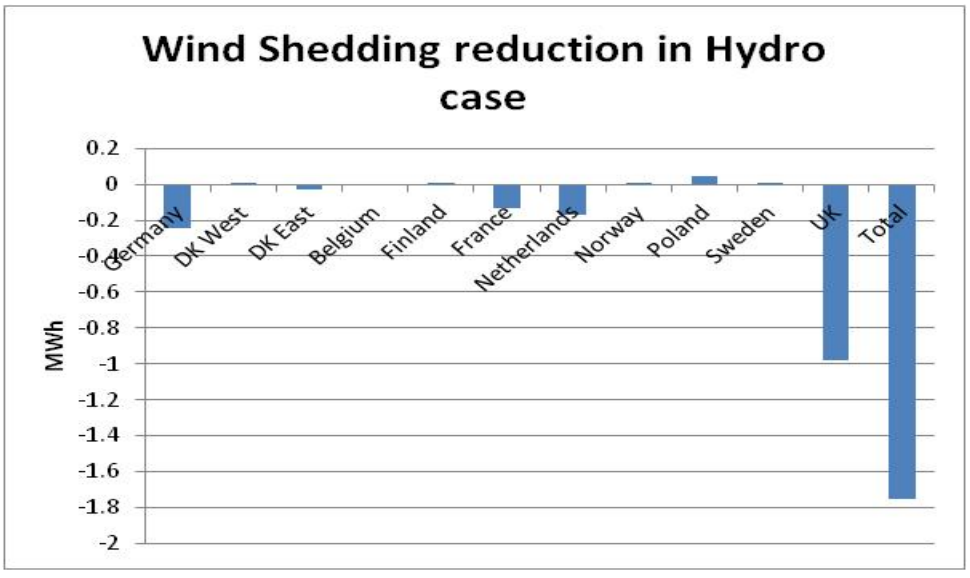


**Figure 51** Wind shedding reduction in Hydro case

It should be noted that the reduction mostly centers around the UK, taking advantage of the new interconnection linking Norway and the UK. This is also to be expected, as the UK represents approximately 63% of the overall wind shedding, so the effect would have been expected to be most pronounced in this region.

### 6.4. Conclusions

Increasing both the hydro capacity and the interconnection capacities have a benefic impact on the overall system. The costs are reduced by a little more than 0,5 B€. The CO2 emissions are also reduced with 10 mil tonnes. Finally, wind power curtailment is reduced with app. 1,5 TWh/year.

| | 2020 | | |
|---|---|---|---|
| **Scenario** | base | hydro | difference |
| **Total costs (M€)** | 36515 | 35997 | 518 |
| **CO2 emission (mil. T CO2)** | 342.5 | 332.6 | 9.9 |
| **Wind shedding (TWh/y)** | 9.4 | 7.9 | 1.5 |

# 7. Impact of new storm controller on COE / emissions

## 7.1. Expected outcomes of this analysis

- Make reference to the KPI's:

| | |
|---|---|
| KPI.16.TF2.10 | Reduction in operational costs in the European power system by 2020 and 2030 assuming new storm control and recommended grid reinforcement to utilise hydro in Nordic system (and the Alps), compared to old storm control and only already planned grid development [Euro/year] |
| KPI.16.TF2.11 | Reduction in CO2 emissions in the European power system by 2020 and 2030 assuming new storm control and recommended grid reinforcements to utilise hydro in Nordic system( and the Alps), compared to old storm control and only already planned grid development [tonne CO2/year] |

## 7.2. Results

WILMAR was also utilized to ascertain the impact of installing the new storm controller on social-economic costs. The benchmark year for wind used has been 2011, when storm impact was moderately significant on system operation, while the rest of the system is configured according to the expected production capacity for 2020. The first output measured was the marginal price in each system region and it is apparent from Table 7.1 that the storm control, by increasing the wind power available is leading to a decrease of marginal costs as expected.

**Table 7.1** Marginal System Prices

| Region | System Average Marginal Price- Base Case (€/MWh) | System Average Marginal Price – Storm Case (€/MWh) | Difference (€/MWh) |
|---|---|---|---|
| **Germany** | 39.62 | 39.56 | -0.07 |
| **Denmark, East** | 11.32 | 10.89 | -0.51 |
| **Denmark, West** | 17.66 | 17.15 | -0.44 |
| **Belgium** | 41.11 | 41.01 | -0.10 |
| **Finland** | 19.26 | 19.03 | -0.23 |
| **France** | 23.19 | 23.10 | -0.09 |
| **Netherlands** | 39.55 | 39.48 | -0.07 |
| **Norway** | 19.00 | 18.74 | -0.25 |
| **Poland** | 40.45 | 40.44 | -0.01 |

| | | | |
|---|---|---|---|
| **Sweden** | 16.53 | 16.30 | -0.23 |
| **UK** | 47.84 | 47.83 | -0.01 |

As it can be seen the effect is most pronounced in the Nordic region, which is expected since the storm controller is only installed in Denmark. As such, the most dramatic drop in marginal prices is in Denmark East, where the price has plummeted by 0.5 €/MWh. This is expected as available wind power, with a marginal price of zero €/MWh is increasing significantly in the Danish regions, as will be shown later.

The same effect can be witnessed when examining the costs of operation for each region, a feature shown in Table 7.2 below. It can be seen that the storm control has had a significant impact on reducing system costs on all fronts; CO2, operation and fuel costs are all reduced by a total of 96 mil. € for the whole of the N. European system.

**Table 7.2 T**otal System Costs before and after storm controller installation

| Regions & Costs (mil. €) | $CO_2$ cost | $CO_2$ cost-Storm Ctl | Fuel cost | Fuel cost-Storm Ctl | OMV cost | OMV cost – Storm Ctl | Total energy cost | Total energy cost – Storm Ctl | Difference |
|---|---|---|---|---|---|---|---|---|---|
| **Germany** | 5266 | 5252 | 6435 | 6420 | 689 | 688 | 12390 | 12360 | -30 |
| **DK West** | 78 | 77 | 138 | 140 | 8 | 8 | 225 | 226 | 1 |
| **DK East** | 62 | 61 | 62 | 61 | 4 | 4 | 128 | 126 | -2 |
| **Belgium** | 113 | 112 | 1160 | 1153 | 355 | 354 | 1628 | 1620 | -8 |
| **Finland** | 69 | 69 | 400 | 397 | 341 | 339 | 810 | 805 | -5 |
| **France** | 421 | 420 | 3822 | 3817 | 4143 | 4139 | 8387 | 8377 | -10 |
| **Netherlands** | 867 | 865 | 1414 | 1408 | 105 | 105 | 2387 | 2378 | -9 |
| **Norway** | 3 | 3 | 12 | 12 | 420 | 417 | 434 | 432 | -3 |
| **Poland** | 2604 | 2598 | 2029 | 2025 | 169 | 168 | 4802 | 4790 | -11 |
| **Sweden** | 73 | 72 | 504 | 497 | 662 | 653 | 1238 | 1221 | -17 |
| **UK** | 3462 | 3462 | 7348 | 7347 | 861 | 861 | 11672 | 11670 | -2 |
| **Total** | 13018 | 12992 | 23325 | 23277 | 7757 | 7737 | 44100 | 44005 | -96 |

While the marginal system price changes were most obvious in Denmark, the system cost reductions are actually mostly located elsewhere and the change is even somewhat positive in Denmark West. The reason for this is the already low marginal system price in Denmark and its small size. As such, the effect is most pronounced in countries like Sweden and Germany who can make savings by reducing their production and reducing exports to Denmark. This is shown in Figure 52 below where the changes in exports from Sweden and Norway to Denmark are depicted.

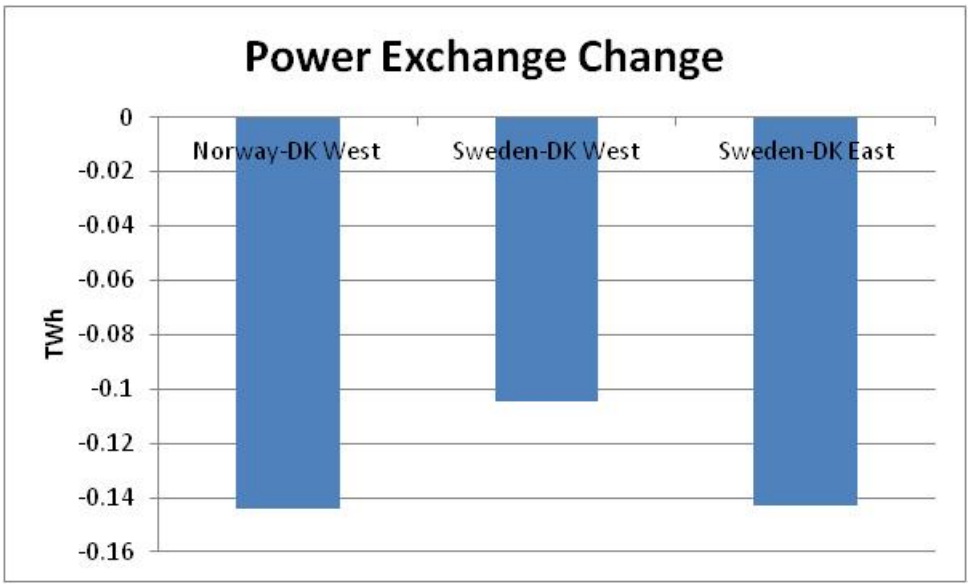


**Figure 52** Export reduction from Sweden and Norway to Denmark

This is also depicted in Figure 53 which shows the changes in production after the installation of the storm controller in each region. Denmark East and West increase their production due to the changes in wind power, while their adjacent regions (Sweden, Norway) reduce their own production as they no longer need to provide as much electricity to Denmark in certain points in time.

This rebalancing in production also explains the widely reduced costs, as the zero-marginal cost wind is replacing expensive fossil fuel or less expensive nuclear production. The changes in the distribution of fuel production are further depicted in Figure 54, where it can be seen that wind is increasing and displacing all other forms of power production, inserting an additional 4,76 TWh into the fuel mix.

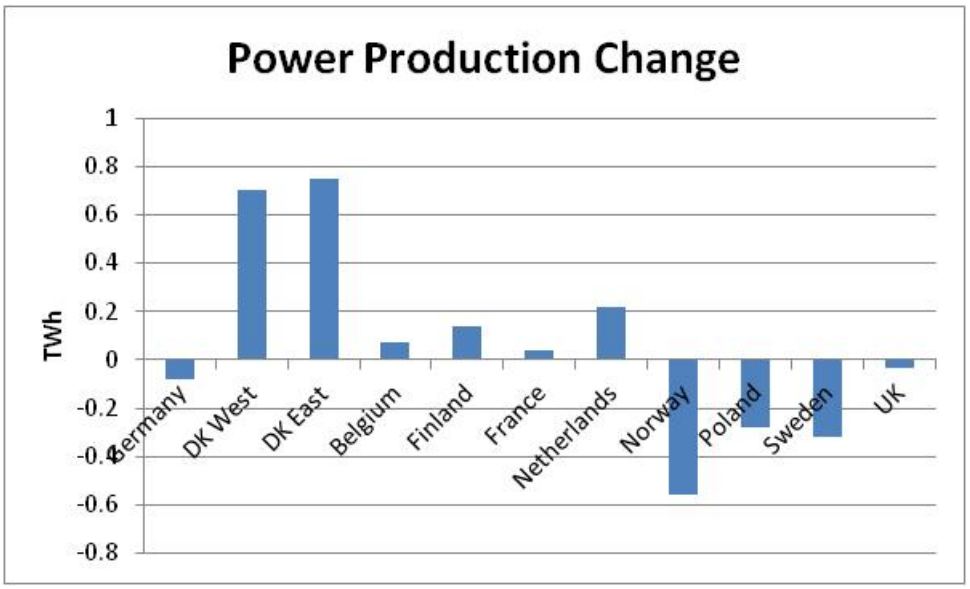


**Figure 53** Change in power production per region

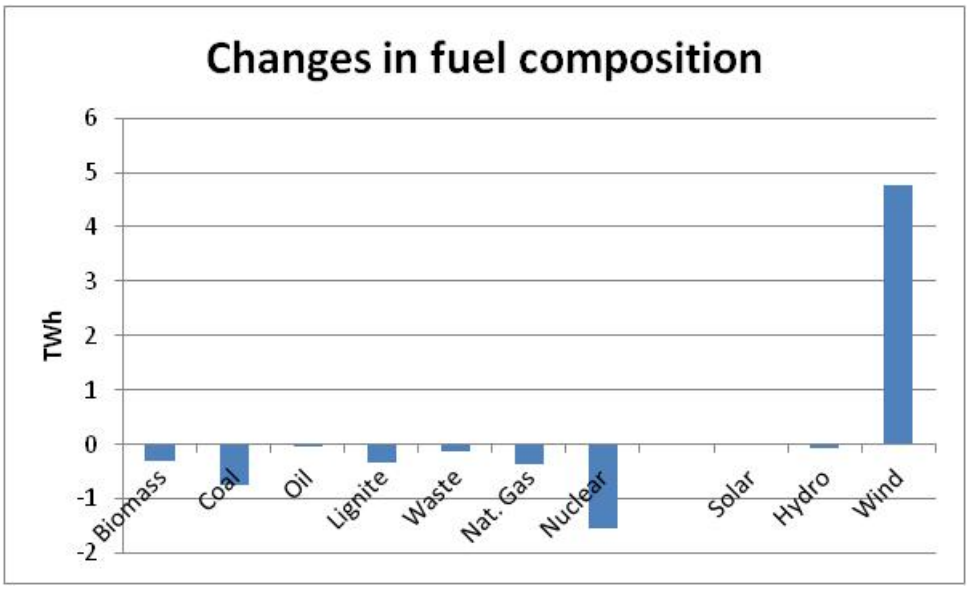


**Figure 54** Changes in fuel composition after storm controller installation

The effect of these changes is to decrease $CO_2$ emissions considerably, as shown in Figure 55 below, always assuming a carbon price of 25 €/ton. Specifically, the sum total of $CO_2$ reduction is approximately 1 million tones of $CO_2$ for the whole N. European System, with the effect being again most pronounced in Germany (almost half of the total change) since its size and high fossil fuel usage leads to big savings even with marginal changes in power production.

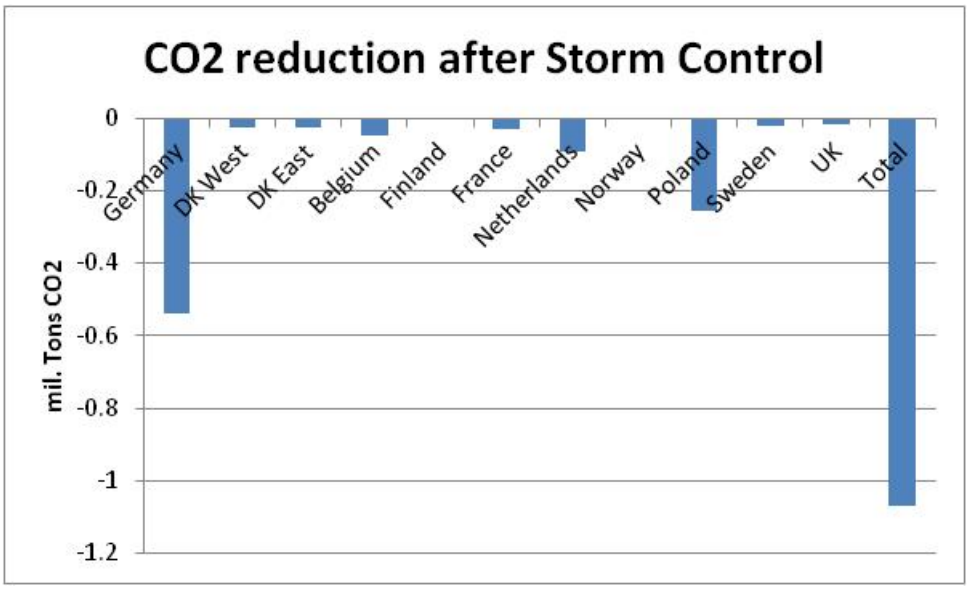


**Figure 55** CO2 reductions after Storm Controller installation

Finally, the increase in total wind power throughout the system has an adverse impact on wind shedding. Considering that storms are likely to happen during periods of already high wind production, it is likely that a not so negligible part of the increased wind production will be shed when optimizing close to zero prices. This is confirmed by Figure 56, where it is shown that the regions with the lowest marginal prices (Denmark East and West) are the ones having the most issues absorbing the surplus wind power.

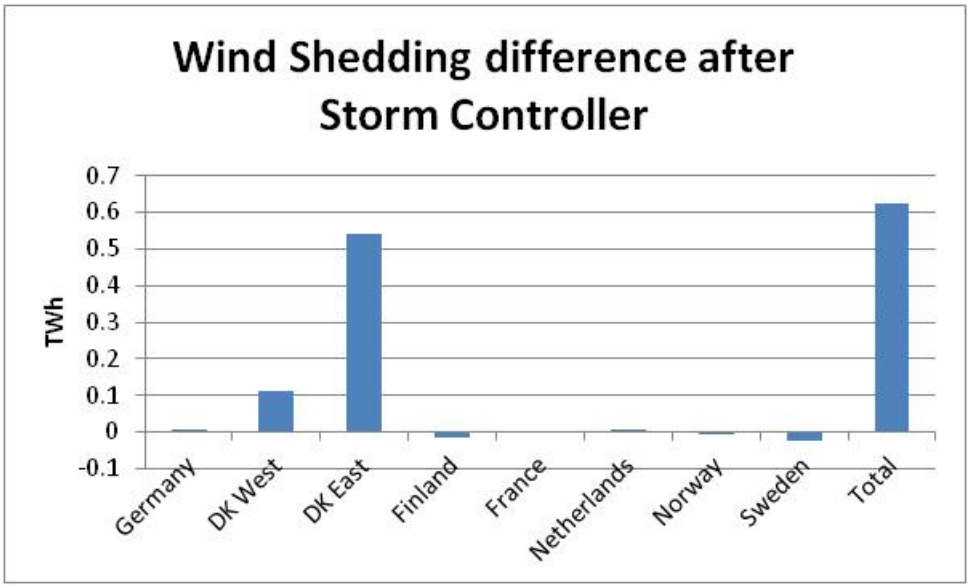


**Figure 56** Wind shedding after Storm Controller installation

In total, the wind shedding is increased by 0.63 TWh, with the entire effect being credited to Danish regions shedding wind. This essentially means that 13.13% of the new wind production is wasted and cannot be absorbed by the market. This percentage is expected to rise as wind penetration increases, but nevertheless shows that the storm control technology can create great benefits even at high wind penetration.

### 7.3. Conclusions

The use of the new storm controller has a positive impact of the overall system. First of all, the wind power production is increased with more than 4TWh/year, even some of it is curtailed. In terms of costs, the overall system costs are reduced with app. 100 M€ and the CO2 emissions are reduced with 1 MTonne.

| | 2020 | | |
|---|---|---|---|
| | HWSD | HWEP | difference |
| **Total costs (M€)** | 44100 | 44005 | 96 |
| **CO2 emission (mil. T CO2)** | 521 | 520 | 1 |
| **Realised wind production (TWh/y)** | 522.76 | 526.88 | 4.12 |
| **Wind shedding (TWh/y)** | 15.85 | 16.48 | 0.63 |

# 8. Overall conclusions

The analysis presented in the report aimed at quantifying the impact that the new storm controller, HWEP, will have on the wind power production if up-scaled to the whole North Europe region. Furthermore, the analysis investigated the reduction in terms of spinning reserves needs to balance the wind power variability. Finally, the importance of different developments in European offshore wind power and availability of flexible hydropower resources for the costs of the power system where analysed and quantified.

The analysis, done at synchronous area level, revealed that the new storm controller will have a positive impact on the wind power forecast error. The improvement is in the range of 10% for the larger synchronous systems in 2020, while the impact seems to be less for 2030.

Being able to control wind power in extreme wind conditions in a manner that is more “grid friendly” will have a positive impact on the operation of the European power system. The analysis shows that there will be reduction in terms of wind power forecast error and in the need for spinning reserves due to wind power.

Analysing the variability of wind power in the four synchronous systems considered revealed that, for 2020, wind power maximum ramping – while significant at times – it does reach values higher than the current dimensioning incidents values. For the 2030 scenario, this is not the case, with the values exceeding – for some systems significantly – the dimensioning incidents values. This indicates that the offshore wind power variability should be considered in frequency stability assessment. This work has not been analysing how this should be done, but one way could be to introduce a variable requirement for frequency containment reserves, depending on the current wind power production.

Increasing both the hydro capacity and the interconnection capacities have a benefic impact on the overall system. The costs are reduced by a little more than 0,5 B€. The CO2 emissions are also reduced with 10 mil tonnes. Finally, wind power curtailment is reduced with app. 1,5 TWh/year.

The use of the new storm controller has a positive impact of the overall system. First of all, the wind power production is increased with more than 4TWh/year, even some of it is curtailed. In terms of costs, the overall system costs are reduced with app. 100 M€ and the CO2 emissions are reduced with 1 MTonne.

## 9. References

[1] N. A. Cutululis, M. Litong-Palima, L. Zeni, A. Gøttig, N. Detlefsen, P. Sørensen, "Offshore Wind Power Data", D16.1, TWENTIES project, 2012, www.twenties-project.eu

[2] R.Veguillas, M.Hermosa, V.McGrail, K. Edlund, Anne-Marie Denis, N.Detlefsen, J.B.Topgaard, N.H. Hansen, C.Druet, J.L. Fernández, M.Lorenzo, V.González, J.García, P.Sørensen, N.A.Cutululis, J.Van den Berg. TWENTIES D2.1. Project Objectives & KPI. December 2010

[3] N. A. Cutululis, A. Hahmann, M.H. Bjerge, A. Gøttig, L.H. Hansen, N. Detlefsen, P. Sørensen, "Assessment of Storm Forecast", D6.1, TWENTIES project, 2011, www.twenties-project.eu

[4] N. Detlefsen, M. Litong-Palima, N.A. Cutululis, H. Farahmand, D. Huertas-Hernando, P. Sørensen, "Report with data for system behaviour at storm passage with original (uncoordinated) and coordinated control", D12.2, TWENTIES project, 2013, www.twenties-project.eu

[5] B. Parson, M. Milligan, B. Zavadil, D. Brooks, B. Kirby, K. Dragoon, J. Caldwell, "Grid Impacts of Wind Power: A summary of recent studies in the United States," Wind Energy (2004), 7, pp 87-108

[6] P. Sørensen,, N.A. Cutululis, A. Vigueras-Rodriguez, L.E. Jensen, J. Hjerrild, M.H. Donovan, H. Madsen. Power fluctuations from large wind farms. IEEE Trans. Power Systems (2007) 22 , 958-965

[7] Operation Handbook. Appendix 1. Load-frequency control and performance. ENTSO-E 16.06.2004. https://www.entsoe.eu/publications/system-operations-reports/operation-handbook/.

[8] Nordic Grid Code (Nordic Collection of Rules). Nordel 2007.

[9] P. Sørensen, A. D. Hansen & P. A. C. Rosas, Wind models for simulation of power fluctuations from wind farms. Journal of wind engineering and industrial aerodynamics 1381–1402 (2002). doi:10.1016/S0167-6105(02)00260-X

[10] W. Wang, C. Bruyere, M. Duda, J. Dudhia, D. Gill, H-C. Lin, J. Michaelakes, S. Rizvi, and X. Zhang. WRF-ARW Version 3 Modeling System User's Guide. Mesoscale & Microscale Meteorology Division, National Center for Atmospheric Research, Boulder, USA, 2009.

[11] G. L. Mellor and T. Yamada. 1982: Development of a turbulence closure model for geophysical fluid problems, Rev. Geophys. and Space Phys., 20, 851-875.

[12] A.N. Hahmann, D. Rostkier-Edelstein, T. T. Warner, Y. Liu, F. Vandenberg, R. Babarsky, and S. P. Swerdlin, 2010: A reanalysis system for the generation of mesoscale climatographies. J. Appl. Meteor. Climatol., 49, 954-972.

[13] A. Pena Diaz, , A. N. Hahmann, C. B. Hasager, F. Bingöl, I. Karagali, J. Badger, M. Badger, N.-E. Clausen, 2011: South Baltic Wind Atlas: South Baltic Offshore Wind Energy Regions Project. / Roskilde, Danmarks Tekniske Universitet, Risø Nationallaboratoriet for Bæredygtig Energi, 66 p. (Denmark. Forskningscenter Risoe. Risoe-R; No. 1775(EN)).

[14] A. N. Hahmann, J. Lange, A. Pena Diaz, C. B. Hasager,, 2012: The NORSEWInD numerical wind atlas for the South Baltic. / DTU Wind Energy, 2012. 53 p. (DTU Wind Energy E; No. 0011(EN)).

[15] D. P. Dee et al., 2011. The ERA-Interim reanalysis: configuration and performance of the data assimilation system. Quart. J. Roy. Meteorol. Soc. 137 (656), 553–597.

[16] J. G. Gonzáles et al, “Economic impact analysis of the demonstrations in task-forces TF1 and TF3”, D15.1, TWENTIES project, www.twenties-project.eu, 2013

[17] IEC 61400-12: Wind-turbine Generator Systems, Part 12:- Wind-turbine Power Performance Testing (2006)

[18] H. Farahmand, S. Jaehnert, T. Aigner and D. Huertas-Hernando, “Possibilities of Nordic hydro power generation flexibility and transmission capacity expansion to support the integration of Northern European wind power production: 2020 and 2030 case studies”, D 16.3, TWENTIES project, www.twenties-project.eu